TEMPORAL DECONVOLUTION OF VASCULAR PLANT-DERIVED FATTY ACIDS EXPORTED FROM TERRESTRIAL WATERSHEDS

Jorien E. Vonk[1,2*], Nicholas J. Drenzek[3†], Konrad A. Hughen[3], Rachel H.R. Stanley[3,4], Cameron McIntyre[2,5,6], Daniel B. Montluçon[2,3], Liviu Giosan[7], John R. Southon[8], Guaciara M. Santos[8], Ellen R.M. Druffel[8], August A. Andersson[9], Martin Sköld[10], Timothy I. Eglinton[2,3]

[1] *Department of Earth Sciences, Vrije Universiteit Amsterdam, Amsterdam, The Netherlands*
[2] *Geological Institute, Eidgenössische Technische Hochschule Zürich, Switzerland*
[3] *Department of Marine Chemistry & Geochemistry, Woods Hole Oceanographic Institution, Woods Hole, US*
[4] *Department of Chemistry, Wellesley College, Wellesley, US*
[5] *Laboratory for Ion Beam Physics, Eidgenössische Technische Hochschule Zürich, Switzerland*
[6] *Scottish Universities Environmental Research Center, Glasgow, UK*
[7] *Department of Geology & Geophysics, Woods Hole Oceanographic Institution, Woods Hole, US*
[8] *Department of Earth System Science, University of California at Irvine, Irvine, US*
[9] *Department of Environmental Science and Analytical Chemistry, Stockholm University, Stockholm, Sweden*
[10] *Department of Mathematics, Stockholm University, Stockholm, Sweden*
†Now at BHGE Oil & Gas Technology Center, Oklahoma City, US

[*] *Corresponding author, j.e.vonk@vu.nl*

ABSTRACT

Relatively little is known about the amount of time that lapses between the photosynthetic fixation of carbon by vascular land plants and its incorporation into the marine sedimentary record, yet the dynamics of terrestrial carbon sequestration have important implications for the carbon cycle. Vascular plant carbon may encounter multiple potential intermediate storage pools and transport trajectories, and the age of vascular plant carbon accumulating in marine sediments will reflect these different pre-depositional histories. Here, we examine down-core ^{14}C profiles of higher plant leaf wax-derived fatty acids isolated from high fidelity sedimentary sequences spanning the so-called "bomb-spike", and encompassing a ca. 60-degree latitudinal gradient from tropical (Cariaco Basin), temperate (Saanich Inlet), and polar (Mackenzie Delta) watersheds to constrain integrated vascular plant carbon storage/transport times ("residence times").

Using a modeling framework, we find that, in addition to a "young" (conditionally defined as < 50 y) carbon pool, an old pool of compounds comprises 49 to 78 % of the fractional contribution of organic carbon (OC) and exhibits variable ages reflective of the environmental setting. For the Mackenzie Delta sediments, we find a mean age of the old pool of 28 ky (±9.4, standard deviation), indicating extensive pre-aging in permafrost soils, whereas the old pools in Saanich Inlet and Cariaco Basin sediments are younger, 7.9 (±5.0) and 2.4 (±0.50) to 3.2 (±0.54) ky, respectively, indicating less protracted storage in terrestrial reservoirs. The "young" pool showed clear annual contributions for Saanich Inlet and Mackenzie Delta sediments (comprising 24% and 16% of this pool, respectively), likely reflecting episodic transport of OC from steep hillside slopes surrounding Saanich Inlet and annual spring flood deposition in the Mackenzie Delta, respectively. Contributions of 5-10 year old OC to the Cariaco Basin show a short delay of OC inflow, potentially related to transport time to the offshore basin. Modeling results also indicate that the Mackenzie Delta has an influx of young but decadal material (20-30 years of age), pointing to the presence of an intermediate reservoir.

Overall, these results show that a significant fraction of vascular plant C undergoes pre-aging in terrestrial reservoirs prior to accumulation in deltaic and marine sediments. The age distribution, reflecting both storage and transport times, likely depends on landscape-specific factors such as local topography, hydrographic characteristics, and

mean annual temperature of the catchment, all of which affect the degree of soil buildup and preservation. We show that catchment-specific carbon residence times across landscapes can vary by an order of magnitude, with important implications both for carbon cycle studies and for the interpretation of molecular terrestrial paleoclimate records preserved in sedimentary sequences.

1. INTRODUCTION

The transfer of organic matter from continents to the sea by rivers (Hedges et al., 1997; Keil et al., 1997; Raymond and Bauer, 2001) and wind (Gagosian and Peltzer, 1986; Conte and Weber, 2002) involves a myriad of processes that collectively are linked to the evolution of Earth's climate through the regulation of carbon, oxygen, and nutrient cycles (Berner, 1989; Crowley, 1995). These processes are likely to also play an important role in future climate change (Fig. 1). Rivers alone supply enough dissolved and particulate organic carbon (DOC and POC, respectively) to the ocean on an annual basis to account for the turnover of all DOC in the oceans and all POC accumulating in underlying sediments, yet little (<10%) land-derived material is found in either reservoir (Martin et al., 2013; Hedges et al., 1997; Schlunz and Schneider, 2000). Although remineralisation is clearly the primary fate of land-derived organic carbon (OC) delivered to the marine environment is remineralisation (Burdige, 2005), implying that only a small portion of the OC derived from terrestrial photosynthesis is buried, this minor "leakage" of carbon from the biosphere to the geosphere forms a significant carbon sink with long-term carbon cycle implications (Galy et al., 2007; Hilton et al., 2015), and yields a valuable window into past dynamics of the terrestrial biosphere.

Organic matter storage within, and transfer between, intermediate pools (e.g., soils or floodplain sediments) likely exerts a strong influence on the overall timescales of transmission of OC from biological source to sedimentary sink, the nature of exported OM as well as the overall efficiency of OC translocation. The non-contemporary (aged, or "pre-aged") radiocarbon signatures (i.e., ^{14}C age older than 1950) of certain DOC and especially POC fractions in an array of soils (Trumbore and Harden, 1997; Lichtfouse, 1999; Rethemeyer et al., 2004; van der Voort et al., 2017), rivers and estuaries (Raymond

and Bauer, 2001; Goñi et al., 2005; Galy & Eglinton, 2011; Tao et al., 2015), and oceanic settings proximal to continental margins (Goñi et al., 2005; Walker et al., 2014; Blair et al., 2004; Drenzek et al., 2007; 2009; Griffith et al., 2010; Tao et al 2016; Bröder et al., 2018) must at least partly reflect these storage and transport times. However, such ^{14}C depletions may also reflect the presence of petrogenic material weathered from ancient sedimentary rocks that has resisted complete destruction by diagenetic and catagenetic forces for millions of years (Yunker et al, 2002; Goñi et al., 2005; Drenzek et al., 2007; 2009; Galy et al., 2008; Hilton et al., 2011; Van der Voort et al., 2017). In contrast to the burial of OC from the terrestrial biosphere, the exhumation and re-burial of petrogenic OC has no net effect on atmospheric CO_2 (Galy et al., 2008). Therefore, differentiating between petrogenic OC and vascular plant OC is crucial in assessing residence times of the latter, and bears directly upon our understanding of carbon cycle processes.

While ^{14}C measurements on bulk OC typically integrate signatures from several OC sources (e.g., vascular plant and petrogenic inputs), isotopic measurements on source-diagnostic organic compounds (biomarkers) enable ^{14}C signatures to be assigned to specific inputs. Plant leaf wax lipids, including long-chain ($\geq$ *n*C_{24}), even-carbon-numbered alkanoic (fatty) acids, are one such example. These biomarkers are almost exclusively produced by higher plants (Eglinton and Hamilton, 1967; Kunst and Samuels, 2003), and inherit the ^{14}C signature of the atmospheric CO_2 from which they are synthesized. Long-chain, odd-carbon-numbered *n*-alkanes have been commonly employed as plant wax biomarkers, and have been extensively investigated in terms of their carbon number distribution and stable isotopic composition (e.g., Wiesenberg et al., 2004; Smittenberg et al., 2006). However, *n*-alkane ^{14}C signatures are sensitive to even trace amounts of petrogenic *n*-alkanes of natural or anthropogenic origin, while *n*-alkanoic acids provide a less contaminated target (van der Voort et al., 2017).

Here, we examine the temporal evolution of $\Delta^{14}C$ signatures of plant waxes (*n*-alkanoic fatty acids) exported from three different terrestrial basins during the course of the 20th century recorded in adjacent aquatic (coastal) sediments. These sites were selected because of their environmental and latitudinal variability, yet relatively stable depositional settings. High accumulation rates coupled with a lack of bioturbation in these settings affords highly precise, independent chronologies by which lipid $\Delta^{14}C$ values can be decay-

corrected to their values at the time of deposition, and then directly compared to well-established historical variations in the radiocarbon content of atmospheric carbon dioxide (CO_2 $\Delta^{14}C$). Comparison with atmospheric CO_2 $\Delta^{14}C$ variations during the period of atmospheric nuclear weapons testing provides a large input signal (Levin and Hesshaimer, 2000) and allows us to quantitatively resolve the fractional abundances and ages of plant wax populations that contribute to the overall apparent residence time of vascular plant OC associated with its translocation from biological source to aquatic sedimentary sink.

2. SETTINGS & METHODS

2.1. Study Sites

The Cariaco Basin, located off of the northern coast of Venezuela, is a tectonic, pull-apart depression consisting of two ca.1400 m deep sub-basins separated by a ca. 900 m deep ridge (Fig. 2a). Its subsurface waters are isolated from the abyssal Caribbean by a shallow (ca. 150 m) sill, allowing only waters from the oxygen minimum zone to infill the deep basin. Strong wintertime trade winds accompanying a southward migration of the Intertropical Convergence Zone (ITCZ) promote upwelling of nutrient-rich waters that fuel high rates of primary production (Astor et al., 2003), while heavy rainfall associated with the northward return of ITCZ during boreal summer increases terrigenous runoff from several rivers (including the Unare, Neveri, Tuy, and Manzanares; Fig. 2a) draining both rainforest and grassy highland in northern South America. Fluvial inputs to the Cariaco Basin are mainly from these local rivers (with the Unare River dominating; Elmore et al., 2009) instead of more distant rivers such as the Orinoco and the Amazon Rivers (Martinez et al., 2007). The Santa Clara dam in the Unare River was built in 1963 (http://www.fao.org/nr/water/aquastat/dams/). The high vertical organic matter fluxes in the Cariaco Basin efficiently strip the remaining oxygen from waters below ca. 300 m (Ho et al., 2004), yielding annually laminated (varved) underlying sediments that are virtually devoid of bioturbation (Hughen et al., 1996). Although lithogenic grains comprise several tens of percent by weight of the total sediment mass (Yarincik et al., 2000), the contribution of terrigenous organic matter to the total organic carbon (TOC) inventory is generally considered to be small (Thunell et al., 2000; and data presented herein). Terrigenous OC

inputs in the basin are dominated by fluvial as opposed to eolian transport (Elmore et al., 2009, Martinez et al., 2010).

The Saanich Inlet is a 26 km long, 8 km wide, ca. 235 m deep coastal fjord in British Columbia, Canada (Fig. 2b), that receives the majority of its freshwater and terrigenous sediment in fall and winter from the Cowichan River located approximately 10 km to the northwest (Blais-Stevens et al., 1997; Tunnicliffe, 2000; Price and Pospelova, 2011). Lesser terrigenous contributions come from the much larger Fraser River (mostly during summer) draining into the Strait of Georgia (Gucluer and Gross, 1964; Hamilton and Hedges, 1988; Tunnicliffe, 2000; Price and Pospelova, 2011) and the small Goldstream River at the head of the fjord itself. The Cowichan River watershed is nearly 800 km^2 in size and originates in Cowichan Lake. The river was modified and channelized (Mclean et al., 2013) in the second half of the last century. Smittenberg et al. (2006) found that soils surrounding the Saanich Inlet are actively accumulating refractory OC, and likely exhibit soil OC turnover times of several thousands of years. The relatively steep topography within these drainage basins is overlain by thick forests of conifers, cedar and oak, characteristic of the cool, moist maritime climate (Pellatt et al., 2001). Deep water ventilation within the Saanich is limited by a ca. 65 m deep sill at the entrance to the fjord, which, combined with high surface productivity, maintains deepwater dysoxia and seasonal anoxia (Anderson and Devol, 1973; Timothy and Soon, 2001), preserving annual varves in sediments below 70–150 m water depth (Gucluer and Gross, 1964). Analysis of lignin oxidation products led Hamilton and Hedges (1988) and Cowie et al. (1992) to conclude that vascular plant debris contributed between 10 and 25% of the TOC in Saanich sediments, while Timothy et al. (2003) put it closer to 40% using bulk elemental and isotopic analyses.

The Mackenzie Delta (Northwest Territories, Canada) is the second-largest Arctic delta (Emmerton et al., 2007), and nearly all of its freshwater (316 km^3/y) and sediments (128 Mt/y) come from the Mackenzie River (Carson et al., 1998; Holmes et al. 2013). The Mackenzie River watershed covers about 1,750,000 km^2, consists of (boreal) forests, wetlands, tundra, and is partly underlain by continuous (16%) or discontinuous (29%) permafrost (Holmes et al., 2013). The delta is covered with >45,000 lakes that efficiently trap sediments and organic matter from the Mackenzie River (Emmerton et al., 2007;

Carson et al., 1998). The main stem of the Mackenzie River is not dammed, but the Peace River, one of the largest tributaries, contains two dams (Bennett Dam, constructed in 1968 and Peace Canyon Dam, constructed in 1980) that have caused significant weakening of the Spring freshet discharge (Woo and Thorne, 2003).

The large differences between the three study sites - a deep oceanic setting, coastal fjord, and arctic delta - and their catchment conditions and climate (mean annual temperature (MAT) ranging from 30°C to -5°C) provide an interesting contrast in studying the characteristics of their terrestrial organic matter export.

2.2. Core sampling and processing

Cariaco Basin sediments from the northwestern flank of the eastern sub-basin were retrieved by a six-barreled multicorer onboard the R/V *Hermano Gines* in May 2004. Three of the cores (CB2, CB5, and CB6) were immediately sectioned at 0.5 cm intervals into pre-combusted glass jars, and stored frozen.

Saanich Inlet depocenter sediments were recovered in August 2003 from the R/V *Clifford Barnes* using a custom-fabricated aluminum freeze corer filled with a dry ice/isopropanol slurry. Core slabs were wrapped in aluminum foil and plastic film and stored frozen. Three of these cores (SI3, SI4, and SI7) were then sectioned into individual varves while still frozen using a band saw equipped with a diamond-coated blade. Core sections were kept frozen during this process by periodic immersion in liquid nitrogen. Each cut varve was transferred to pre-combusted glass jars and stored frozen until analysis, with turbidites (see section 2.3) archived as a whole unit.

Mackenzie Delta lake sediments were retrieved from ice-covered lake LD-1 in the lower delta in March 2007 and March 2009 using piston coring (system built in-house at Geology and Geophysics, Woods Hole Oceanographic Institution (WHOI), core diameter 2 and 3 inch). Coring locations were selected using ground penetrating radar surveys that aimed for lakes with water depths greater than 2.5 m, and away from lacustrine deltas. Cores were shipped in cooled conditions, and split lengthwise. The 2007 core (84cm; MK07#6) was used for bulk organic geochemical analysis, and the 2009 core (187cm; MK09#2) was used for radioisotopic measurements (one half), and molecular isotopic analysis (other half, sectioned into 1-cm slices).

212

213 **2.3. Chronology development**

214 Select horizons from Cariaco multicores CB2, CB5, and CB6 and Saanich freeze
215 core SI3 were freeze dried, pulverized, and analyzed for ^{210}Pb and ^{137}Cs activity via gamma
216 spectroscopy. For Cariaco Basin sediments, a ^{210}Pb–based mean sedimentation rate of 0.1
217 cm yr^{-1} was calculated based on:

218 $$S = -\lambda / \text{slope} \quad (1)$$

219 where S is the sedimentation rate, λ the decay constant of 0.031 yr^{-1} and the slope is taken
220 from the plot of ln^{210}Pb-xs (excess Pb) against depth (Fig. 3b). This was anchored to the
221 (assumed) 1963 maximum in atmospheric ^{137}Cs fallout (Robbins et al. 2000) (although
222 likely the sediment deposition was not until 1964; Klaminder et al., 2012) (Fig. 3a). The
223 ^{137}Cs peak was 0.5 cm lower in both CB2 and CB6; thus individual sedimentary horizons
224 from these cores were combined with those from one level higher in CB5 to yield sufficient
225 biomarker quantities for ^{14}C analysis.

226 For Saanich Inlet sediments, the freeze cores were photographed and
227 stratigraphically correlated with one another via enumeration of individual varves – each
228 visually consisting of one light lamina from a succession of spring/summer diatom blooms
229 and one dark lamina from terrigenous runoff in the autumn/winter – as well as through the
230 comparison of episodic, earthquake-emplaced turbidite deposits (Blais-Stevens et al.,
231 1997). Depth from the top and bottom of one particularly large turbidite to the base of each
232 varve above and below it, respectively, was carefully noted to aid the development of an
233 ancillary ^{210}Pb and ^{137}C-based chronology. The chronology above and below the ^{137}Cs
234 spike in SI3 was principally established by annual varve counting, indicating that the
235 uppermost and lowermost horizons were deposited in 1987 and 1810 CE, respectively (Fig.
236 4a). This approach yielded an average sedimentation rate of 0.85 cm yr^{-1}, in reasonable
237 agreement with a value of 1.0 cm yr^{-1} calculated from the ^{210}Pb profile (Fig. 4b). This also
238 fits with previous varve counting in two 6000-year cores in Saanich Inlet (Nederbragt and
239 Thurow, 2001) showing recent annual varve thicknesses between 0.75 and 1.25 cm. For
240 our cores, individual varves representing the same year in SI3, SI4, and SI7 were then
241 combined for biomarker ^{14}C analysis.

Horizons from Mackenzie Delta sediment core MK09#2 were analyzed for ^{137}Cs activity, as described in Vonk et al. 2015 (MK09#2 indicated with LD-1). Briefly, the onset of ^{137}Cs activity (corresponding to 1951) was observed at 60 cm depth, the peak (corresponding to 1963 or 1964; Robbins et al., 2000; Klaminder et al., 2012) at 52.5 cm, which resulted in a sedimentation rate of 1.17 cm yr-1 for 1964-2009 and 0.58 cm yr-1 for 1951-1964 (Fig. 5). These sedimentation rates were corroborated with lamina counting (Vonk et al., 2015).

2.4. Bulk isotopic analyses

Cores CB6, SI3, and MK07#6 were also profiled for total carbon (TC), total nitrogen (TN), and TOC (following the removal of carbonate minerals via gaseous and aqueous 2N hydrochloric acid treatment at 60-65°C) by high temperature combustion on a Carlo Erba 1108 Elemental Analyzer. TOC $\delta^{13}C$ and $\Delta^{14}C$ values were measured following established protocols at the National Ocean Sciences Accelerator Mass Spectrometry (NOSAMS) facility at WHOI (McNichol et al., 1994). Details of the method for analysis of MK09#2 are also described in Vonk et al., 2015.

2.5. Molecular isotopic analyses

Sediments from Cariaco Basin and Saanich Inlet were extracted and isolated at the Department of Marine Chemistry and Geochemistry (at WHOI) and analyzed at the NOSAMS facility at WHOI, whereas sediments from the Mackenzie Delta (MK09#2) were extracted and isolated at the Geological Institute (ETH-Zürich) and analyzed at the AMS facility of the Laboratory of Ion Beam Physics (ETH-Zürich).

2.5.1 Extraction and work-up

Remaining sediments from Cariaco Basin cores CB2, CB5, and CB6 and Saanich Inlet cores SI3, SI4, and SI7 were combined into chronologically equivalent horizons. These horizons were spiked with several internal standards of known $\delta^{13}C$ and $\Delta^{14}C$ composition and extracted in dichloromethane (DCM):methanol 9:1 v/v with an Accelerated Solvent Extraction (ASE) system. The resulting extract was dried over $NaSO_4$, solvent-exchanged into hexane, and chromatographically separated into different

fractions using glass columns packed with fully activated silica gel and elution with successive additions of the following solutions (v/v): f1 = hexane, f2 = 50/50 hexane/toluene, f3 = 80/20 hexane/diethyl ether, f4 = 75/25 hexane/ethyl acetate, f5 = 99.85/0.15 diethyl ether/acetic acid, and f6 = methanol. The f5 fraction contained unesterified or "free" acids and was further purified by solvent-exchanging into DCM and passing through smaller glass columns containing aminopropyl-doped silica gel with f1 = 15 mL of 90/10 DCM/acetone, f2 = 20 mL of 98/2 DCM/formic acid, and f3 = 15 mL of methanol. Free fatty acids in the f2 fractions from this second chromatographic step were then esterified overnight in a solution of 95/5 anhydrous methanol/hydrochloric acid of known carbon isotopic composition. The corresponding fatty acid methyl esters (FAMEs) were subsequently extracted into hexane, re-dried over sodium sulfate, and further purified by elution through Pasteur pipette columns containing 5 % (wt.) deactivated silica gel with f1 = 4 mL hexane, f2 = 4mL 95/5 hexane/ethyl acetate, and f3 = 4mL methanol. Each resultant f2 fraction was then solvent-exchanged into a known volume of hexane and injected along with authentic standards on a Hewlett Packard (HP) Series II gas chromatograph (GC) equipped with a flame ionization detector (FID) to measure individual FAME abundances. Compound-specific $\delta^{13}C$ analyses on all even carbon-numbered homologues between n-C_{16} and n-C_{32}, along with a co-injected n-C_{36} alkane standard of known isotopic composition, were performed in triplicate on a HP 6890 GC coupled to a Finnigan Delta^{plus} isotope ratio mass spectrometer (GC/IRMS) via a modified combustion interface.

Sediments of MK09#2 (Mackenzie Delta) were freeze-dried and extracted as 1-cm core horizons (5-7 gram per horizon) in 10-15mL DCM:methanol 9:1 v/v using a MARS unit from CEM operated at 1700W and 100°C for 20 minutes. Microwave vessels were blank-extracted prior to sample introduction. The total lipid extracts were dried under N_2 and saponified with 0.5 M potassium hydroxide in methanol at 70°C for 2 h. After addition of 5-10 mL Milli-Q water-salt (sodium chloride) solution the 'neutral' fraction was obtained through back-extraction with hexane, and subsequently, an 'acid' fraction was obtained after acidification down to pH 2 (with concentrated hydrochloric acid) and back-extraction with hexane:DCM 4:1 v/v. The acid fraction was derivatized with BF_3-methanol for 30 min at 80°C, and back-extracted with DCM after addition of Milli-Q water. The resulting

FAME fraction was further purified onto a 5 % (wt.) deactivated silica gel Pasteur pipette column topped of with sodium sulfate and eluted with (1) hexane, (2) hexane:DCM 4:1 v/v, and (3) DCM. Fraction 2, containing FAMEs, was injected along with authentic standards on a GC-FID (7890A, Agilent Technologies) to check purity.

2.5.2 Isolation and ^{14}C analysis of individual compounds

For Cariaco Basin and Saanich Inlet samples, individual nC$_{16}$, nC$_{24}$, nC$_{26}$, and nC$_{28}$ homologues, as well as the nC$_{14+18}$ and nC$_{30+32}$ homologue combinations, were isolated for ^{14}C analysis by preparative capillary gas chromatography (PCGC) and subsequently combusted to CO_2 using standard techniques (Eglinton et al., 1996). A subset of samples ranging in mass from 31-102 μgC was converted to graphite with a powdered cobalt catalyst and analyzed by standard small sample procedures at NOSAMS (Pearson et al., 1998). Remaining samples of 5-63 μgC were graphitized over iron powder within specially designed reactors containing magnesium perchlorate desiccant and analyzed at the Keck Carbon Cycle Accelerator Mass Spectrometry facility (KCCAMS; see Santos et al. 2007a,b for detailed methods). In order to compensate for the proportional increase in procedural blank contamination at the ultra-small sample level (i.e. < 25 μg carbon; Santos et al., 2010), a solution of standards whose isotopic compositions encompass the full range of Δ^{14}C values (nC$_{19}$ alcohol, Δ^{14}C = –999 ‰; nC$_{21}$ fatty acid, Δ^{14}C = –389 ‰; *iso*-C$_{21}$ fatty acid, Δ^{14}C = –32.9 ‰) was added to separate pre-combusted aliquots of sea sand in several mass increments over this range, extracted, isolated into individual compounds, graphitized, and analyzed on the same KCCAMS wheels according to the procedures described above. Twelve oxalic acid I (NIST SRM 4990B) and eight, neat nC$_{19}$ alcohol standards of similarly varying mass were also combusted, graphitized, and co-analyzed in order to assess blank contributions from these steps alone. Detailed mathematical treatment of all blank corrections can be found in Santos et al. (2007b; 2010). Total masses and mass errors of modern and "dead" (^{14}C-free) blank carbon calculated under this approach were 0.8 ± 0.4 μg (all derived from graphitization as well as combustion) and 1.0 ± 0.5 μg (75% derived from the sample preparation steps preceding combustion), respectively, and are applied to the molecular Δ^{14}C results reported below.

For Mackenzie Delta sediments, long-chain fatty acids were isolated individually (nC$_{20}$, nC$_{22}$, nC$_{30}$ homologues) or in combinations (nC$_{16+18}$ and nC$_{24+26+28}$) using PCGC (Feng et al., 2015; Tao et al., 2015; Vonk et al., 2014). Isolated fractions were eluted using DCM through a silica gel column (1% deactivated), and run on a GC-FID to detect impurities (all <5%). The nC$_{30}$ and nC$_{24+26+28}$ fractions were combined and transferred to pre-combusted quartz-tubes, and gently evaporated under N_2. After addition of precombusted CuO, the tubes were flame-sealed under vacuum, combusted at 850 °C for 5 h, and the resulting CO_2 (7.7 to 22 µg) was cryogenically purified and quantified before analysis on a miniaturized radiocarbon dating system (MICADAS) at the Laboratory of Ion Beam Physics at ETH-Zürich using a gas feeding system (Wacker et al., 2013). We did unfortunately not assess blank values. However, calculations using a later processing blank from the same PCGC and AMS laboratory (Tao et al., 2015) resulted in blank-corrected values that fell within error of the uncorrected values, and would not have changed our interpretations.

All of the $\Delta^{14}C$ results, given in ‰ and reported relative to standard Oxalic II (NIST SRM 4990C), are corrected for the ester methyl group addition from the derivatization agent via an isotope mass balance.

3. RESULTS

3.1. Bulk geochemical data

Sedimentary TOC is about twice as high in the Cariaco Basin at (6.0-6.5%) than in the Saanich Inlet (ca. 3.0%), whereas the Mackenzie Delta exhibits the lowest and most stable TOC values (ca. 1.3%; Fig. S1a). The TOC/TN ratios of the Cariaco Basin (between 7.5 and 10) and Saanich Inlet (ca. 10) are lower than those of the Mackenzie Delta (10.5-12), consistent with higher contributions from marine or coastal biomass for the two former systems. The TOC/TN ratios of Mackenzie Delta sediments show a slight decrease downcore, likely indicative of diagenetic processes. There are no systematic down-core trends in either TOC or TOC/TN in Cariaco sediments, indicating that the overall flux and provenance of organic matter are in approximate steady state relative to the 100-year timeframe considered. In the Saanich Inlet, however, the TOC/TN profile varies in a more systematic fashion (Fig. S1b), with low ratios in the 1920s and 1930s, transitioning to

higher ratios during the mid 1940s, 1950s, 1970s, and 1980s, and a sharp decline just before the 1990s.

The down-core bulk $\delta^{13}C$ signatures ($\delta^{13}C_{TOC}$) of the three sites correspond with the increasing marine and decreasing terrestrial character when going from Mackenzie Delta (ca. -26.4‰ showing a greater influence of C_3 vascular plant-derived OC) to Saanich Inlet (ca. -22 to -23‰), to Cariaco Basin (ca. -20‰, consistent with predominantly marine OC) (Fig. S1c). This gradient from terrestrial to marine dominance is also corroborated by the TOC/TN ratios. The $\Delta^{14}C$ signatures of TOC ($\Delta^{14}C_{TOC}$) show a sharper contrast between the three sites, with relatively modern values for the Cariaco Basin (between -90 and 50‰) and Saanich Inlet (between -225 and -80‰), and low values for the Mackenzie Delta sediments (between -750 and -800‰) (Fig. S1d). The down-core $\Delta^{14}C_{TOC}$ profiles at the two "younger" sites generally trend toward more positive values towards the present, reflecting biosynthetic incorporation of ^{14}C-enriched atmospheric CO_2 and ocean mixed layer DIC associated with the bomb effect (Levin and Hesshaimer, 2000). The $\Delta^{14}C_{TOC}$ profile of the Mackenzie Delta core does not show the positive trend, yet does show an enrichment of the signal from ca. 1970 to 1975, perhaps indicative of a lag in the bomb effect.

3.2. Molecular geochemical data

In the Cariaco Basin, fatty acid $\delta^{13}C$ values remain between ca. -22 to -24 ‰ for n-C_{14} through n-C_{26} homologues, and then decrease rapidly towards n-C_{32} (Fig. S2, S3). While there is also a sharp isotopic contrast between short and long-chain fatty acids in Saanich Inlet sediments, the isotopic shift occurs in two steps, with intermediate chain-length homologues (n-C_{20} – n-C_{26}) consistently displaying intermediate $\delta^{13}C$ values (Fig. S3). Unfortunately, *n*-alkanoic acid $\delta^{13}C$ analyses could not be performed on the MK09#2 Mackenzie Delta core (due to low C concentrations, we prioritized ^{14}C analyses), however Drenzek et al. (2007) reported a 4-5 ‰ difference between $\delta^{13}C$ values of short (n-C_{14}-C_{16}-C_{18}, -25 to -29‰) and long (n-C_{24}-C_{26}-C_{28}, -29 to -33‰) in Beaufort shelf sediments in front of the Mackenzie Delta.

Long-chain fatty acid $\Delta^{14}C$ values are lower with increasing chain length, from ca. 65‰ (n-C_{24}) to -250‰ (n-C_{30+32}) for the Cariaco Basin, and -100‰ (n-C_{24}) to -290‰

(nC$_{30+32}$) for the Saanich Inlet (Table S3a, Fig. 6). Long-chain fatty acid homologues were combined for the Mackenzie Delta sediment core due to low abundance of individual chain lengths (sum of nC$_{24-26-28-30}$), and their composite ^{14}C signature (between -630 and -430‰) was significantly lower (older) than corresponding composite ^{14}C values of the Saanich Inlet (ca. -220‰) or the Cariaco Basin (between -160 and 10‰) (Table S3a, b).

3.3 Model development and description

The analyzed lipid biomarkers in our sampled sediment cores consist of a mixture of components with different "reservoir ages" reflecting their prior storage and transport history. In order to quantitatively resolve the fractional contribution of these reservoir ages, we use a model that considers components that are deposited at time t, with t increasing back in time. Our model is related to approaches used in other studies (Harrison, 1996; Tegen and Dörr, 1996; Mills et al., 2013), except that we use molecular markers instead of bulk soil OC and are therefore able to trace their storage and transport pathways more specifically. We denote the proportions of material with residence time τ in these samples by $f_t(\tau)$ and this proportion's contribution to the observed lipid biomarker $\Delta^{14}C$-signal by $\Delta^{14}C(t,\tau)$. By mass-balance, the signal at time *t* of the sample is then:

$$\Delta^{14}C(t) = \int_0^{\infty} \Delta^{14}C(t,\tau) \cdot f_t(\tau)\, d\tau. \qquad [1]$$

To ensure that the terms in equation [1] are identifiable, we make several assumptions:

(i) The petrogenic contribution to long-chain fatty acid markers is zero (i.e., there is no additional reservoir of ^{14}C-dead material);

(ii) The year of sedimentary deposition is known;

(iii) Bioturbation does not compromise the sediment record;

(iv) The proportions of different soil reservoirs are constant over deposition times t, i.e. $f_t(\tau) = f(\tau)$.

(v) The signal $\Delta^{14}C(t,\tau)$, corresponding to deposition time t and residence time τ, can be decomposed into the atmospheric CO_2 signal at the time of deposition and radioactive decay as:

$$\Delta^{14}C(t,\tau) = \Delta^{14}C_{CO_2}(t+\tau) + 1000 \cdot (e^{-(\tau+t-t_0)\lambda} - 1) \quad [2]$$

where t_0 is the time of analysis of the sample and $\lambda = 1/8267yr^{-1}$ is the radioactive decay rate of Δ^{14}C.

Inserting equation [2] into equation [1], we get:

$$\Delta^{14}C(t) = \int_0^\infty \Delta^{14}C_{CO_2}(t+\tau) \cdot f(\tau)\, d\tau + 1000 \cdot (\int_0^\infty e^{-(\tau+t-t_0)\lambda} \cdot f(\tau)\, d\tau - 1) \quad [3]$$

where we used $\int_0^\infty f(\tau)\, d\tau = 1$ by mass-balance. In this equation, the function f represents the frequency distribution of material with deposition time τ. Based on data at deposition times $t_1, \ldots, t_n$ (in increasing order; t_n representing the deepest measurement depth in the core) we can make the following inferences about f:

1. By tracing the delayed input from the "bomb-spike" in the observed signal, we can use its timing and amplitude to make inference about the "shape" of $f(\tau)$ for $0 \leq \tau \leq t_{bomb} - t_1$ under the assumption that the atmospheric signal is zero for $t > t_{bomb}$.

2. Using data deposited at $t > t_{bomb}$ (i.e., prior to 1963), we may estimate an average level of radioactive decay, which in turn could be used to infer longer residence times. As a detailed inference on $f(\tau)$ for $\tau > t_{bomb} - t_1$ is not possible due to the lack of data points (i.e. lack of variability within the signal), we chose to introduce a single deposition time τ_{Old} representative for older (before the bomb-spike) material in the catchment. The residence time of this material is so long that it is not affected by the bomb ^{14}C inputs over the period 1963 to present. This material is older than 50 years and can be centennial and/or millennial in age. The second term of equation [3] can then be approximated by $1000 \cdot (\exp(-\tau_{Old} \cdot \lambda) - 1) \cdot f_{Old}$, where f_{Old} is the proportion of material with deposition time τ_{Old} and hence $\int_0^{t_n - t_{bomb}} f(\tau)\, d\tau = 1 - f_{Old}$.

Since $\Delta^{14}C$ values from the Mackenzie Delta show a clear decreasing trend prior to the bomb-spike (highlighted in Fig. 6a), presumably reflecting either the "Suess effect" (Levin and Hesshaimer, 2000) and/or a potential recent increase of old OC release from the catchment, we chose to add a linear term outside the mass-balance equation starting at calendar year 1900 (50 years BP). This term with slope b has also been applied for the Cariaco Basin and Saanich Inlet sediment data except from the $C_{30\text{-}32}$ Cariaco Basin data due to limited data resolution before 1950.

Our final model for sample data is then:

$$\Delta^{14}C_{obs}(t_i) = \int_0^{t_{bomb}-t_i} \Delta^{14}C_{CO_2}(t_i+\tau)\cdot f(\tau)\,d\tau + 1000(e^{-\tau_{Old}\cdot\lambda}-1)\cdot f_{Old} + b\cdot (t-50) + \epsilon_i \quad [4]$$

for $i = 1, \dots, n$, where ϵ_i is a normally distributed (Gaussian) measurement error. Parameters to be estimated from this relation are $f(\tau)$ (for $0 \le \tau \le t_{bomb} - t_1$), τ_{Old}, f_{Old}, and the slope b of the linear term. Residence time τ is reported in calendar years, as it is derived from the core chronology (based on ^{137}Cs and ^{210}Pb). Note that material with residence time τ larger than $t_{bomb} - t_1$, but not sufficiently large to show substantial radioactive decay, will not be detected by the current resolution of data since this leaves $\Delta^{14}C(t_i, \tau) \approx 0$ for all i.

To facilitate comparison between the different sites, we choose to estimate f for $0 \le \tau \le 50yrs$ for all three sediment core data. For the Mackenzie Delta sediments, we used ^{14}C values of the combined fraction of $C_{24-26-28-30-32}$ *n*-alkanoic acids and for Cariaco Basin and Saanich Inlet sediment we used ^{14}C values of $C_{26-28-30-32}$. For Cariaco Basin we also analysed C_{30-32} separately, which was not done for Saanich Inlet since those series only consisted of two observations. Note that it is only data from Mackenzie that contains sufficiently recent (t<50 years) data to estimate f in the higher ends of this interval at any resolution.

Best-fit curves were determined (Fig. 7) by minimizing the average residuals between calculated and measured $\Delta^{14}C$ *(t)* values (that have been corrected for decay in sediments) as a function of the remaining variables. We followed a Bayesian approach,

fitting the model using Markov chain Monte Carlo (Clark and Gelfand, 2006) with software JAGS run from the R computing environment. Best-fit curves were determined (Fig. 7) as posterior means computed from the Markov chain Monte Carlo samples. We judged an observation to be a potential outlier (with respect to the model) if it deviated by more than three standard deviations from the estimated mean curve (Fig. 7). Note that this definition includes extreme values as well as observations where the standard deviation of the curve is severely underestimated. In order to check the influence of outliers, they were sequentially removed from the analysis until the results were free from outliers. Saanich Inlet was free from outliers after removing data from 1959 and Mackenzie Delta after removing data from 1906, 1978 and 2005. For these sites, results without outliers were broadly similar to those with outliers (see Supplementary Online Material, Figs. S5, S6, S7). For the $C_{26+28+30+32}$ best-fit curve of Cariaco Basin, either 1971 or 1976 can be considered as an outlier. Removing these points resulted in similar parameters related to the old pool, but, after removal of the 1971 outlier, the temporal distribution of the young pool shifted (see Supplementary Online Material). We also determined best-fit curves without including parameter b (the linear term) but the fit was not as good as the best-fit curve where this parameter was incorporated (Fig. S8, Fig. 7).

4. DISCUSSION

4.1 Organic matter characterization

Whereas ratios of TOC/TN seem to be relatively consistent downcore for both Mackenzie Delta, as well as Cariaco Basin sediments, the TOC/TN profile for the Saanich Inlet exhibits stronger variability (Fig. S1b). This behavior might reflect non-steady state organic matter input to Saanich sediments, something that our model cannot take into account, unfortunately, such as periods of enhanced soil erosion in the latter half of the 20th century as a consequence of large-scale deforestation from the late 1800s through 1960 (Tunnicliffe, 2000). The Saanich Inlet may be sensitive to the location and small size of the Cowichan watershed (795 km^2) that drains into it, which would experience multi-annual oscillations from large-scale weather patterns – such as the El Niño-Southern

Oscillation (ENSO) – that could influence both marine production and terrigenous runoff (McQuoid and Hobson, 1997; Dean and Kemp, 2004).

The Mackenzie River watershed holds relict, petrogenic source rock material that affects the ^{14}C-OC ages (Vonk et al., 2015; Yunker et al., 2002), which is reflected in our bulk ^{14}C signatures of TOC (between -750 and -800‰ for Mackenzie Delta compared with -90 to -50‰ for Cariaco Basin and -225 to -80‰ for the Saanich Inlet; Fig. S1d). The differences between the catchments also likely indicate that the Saanich Inlet and the Mackenzie Delta have a relatively high inflow of aged (by up to several thousand years) biospheric, terrestrial OC. This is supported by earlier published ^{14}C ages of 6500 years BP for long-chain *n*-alkanes at Saanich Inlet (Smittenberg et al., 2006), or biospheric OC ages of 5800 to 6100 years BP for the Mackenzie Delta (Vonk et al., 2015, and Hilton et al., 2015).

At the molecular level, fatty acids from all sites exhibit bimodal abundance distributions of short ($\leq$ *n*C$_{20}$) and long ($\geq$ *n*C$_{24}$) chains, with maxima at *n*C$_{16}$ and *n*C$_{24}$ or *n*C$_{26}$ (see supplementary Table S1; S2, Fig. S2) that typically reflect contributions from autochthonous primary and secondary production (algal/bacterial biomass) and allochthonous higher plant leaf wax inputs, respectively. Although extracts from leaf surfaces exhibit similar distribution patterns (Chikaraishi and Naraoka, 2006), it is generally assumed that faster degradation rates for the short-chain homologues (e.g., Canuel and Martens, 1996) results in efficient replacement of these compounds during fluvial transport with those emanating from autochthonous sources (Gong and Hollander, 1997; Tao et al., 2016). Corresponding δ^{13}C and Δ^{14}C compositions can be used to further constrain sources since (a) δ^{13}C values of individual lipid homologues synthesized by the same aquatic or terrestrial plant species generally vary by no more than a few per mil (Collister et al., 1994; Chikaraishi et al., 2006), and (b) all biomolecules inherit the (fractionation-corrected) Δ^{14}C value of the carbon substrate from which they were synthesized (Pearson, 1999). Because this study focuses on constraining the terrestrial reservoir ages, we focus most of the following discussion on the long-chain ($\geq$ *n*C$_{24}$) *n*-alkanoic acids, because these compounds are almost exclusively higher plant leaf waxes. Concentrations of the shorter homologues, as well as their δ^{13}C and Δ^{14}C molecular signatures can be found in the supplementary information (Table S1; S2, Figs S2, S3).

The difference in $\delta^{13}C$ trends (Fig. S2) with fatty acid chain lengths for Cariaco Basin (a gradual decrease from -22‰ to -24‰ towards -32‰) and Saanich Inlet (a two-step decrease from around -22‰ to -27‰, and then to -32‰) may reflect different species of terrigenous and aquatic plants (Collister et al., 1994), seasonality, diagenetic fractionation (Chikaraishi et al., 2006), and/or varying amounts of algal (Ratnayake et al., 2005) or bacterial (Gong and Hollander, 1997) components. The clear depletion of long-chain fatty acid $\Delta^{14}C$ values with increasing chain lengths (Table S3a) implies that OC in terrestrially-influenced aquatic sediments contains both contemporary or recently produced vascular plant OC (soil litter/plant debris), as well as aged terrestrial OC (e.g., from mineral soils), with the proportions of the components, and the age of the latter, varying with location. As noted by others, release of terrestrial OC previously stored in catchment reservoirs is an important source pathway (Smittenberg et al., 2006, Vonk et al., 2015, Hilton et al., 2015, Tao et al., 2015, Feng et al., 2013).

The individual $\Delta^{14}C$ values of the long-chain homologues at any point in time will represent a composite of different populations of molecules that have been aged to varying degrees as they follow different transport trajectories and pass through a broad continuum of terrigenous reservoirs (Fig. 1). Further insights into the underlying processes can be attained when these molecular isotopic profiles are considered in relation to each other and to the atmospheric bomb-spike (Hua et al., 2013). First, all long-chain fatty acids in both records are markedly lower in ^{14}C relative to atmospheric CO_2, with the magnitude of depletion systematically increasing with increasing chain length (Fig. 6b, c). This is a general trend that has been observed in other molecular-level radiocarbon studies of sedimentary fatty acids (Pearson, 1999; 2001; Uchida et al., 2001; Ohkouchi et al., 2003; Drenzek et al., 2007, 2009), yet the underlying cause(s) of this phenomenon remains unclear. It may be an artifact of mixing between the $\Delta^{14}C$ signatures of long-chain homologues derived from autochthonous and allochthonous production. Alternatively, slower degradation rates for longer-chain homologues (Canuel and Martens, 1996) might allow for protracted storage in intermediate reservoirs. The latter scenario appears to be more consistent with the observation of the same $\Delta^{14}C$ trend in an aerosol sample from Japan (Matsumoto et al., 2001). Third, greater hydrophobicity of the longer chain homologues may promote their association with mineral matter in soils, lakes, and river

568 beds, thereby rendering them more resistant to degradation, as well as to leaching and
569 aqueous transport. Irrespective of which of the above applies, and in the absence of
570 bioturbation, the discrepancy between $\Delta^{14}C$ values of the long-chain FAs relative to that of
571 more modern mixed layer DIC indicates their origin is unrelated to marine
572 photoautotrophy. Together with their corresponding stable carbon isotopic compositions,
573 these observations imply a significant contribution of aged vascular plant waxes to
574 sediments at each of the three investigated sites.

575 Despite the overall depletion in ^{14}C relative to atmospheric CO_2, the incorporation
576 of bomb radiocarbon is reflected in the ^{14}C enrichments displayed by long-chain
577 homologues extracted from post-1950 sediments over those from pre-1950 horizons. In the
578 Cariaco Basin, maximum values in all fatty acid homologues do not occur until the
579 early/mid-1970s (Fig. 6a, c), a period when the ^{14}C content of the atmosphere was already
580 in decline. Moreover, minimal enrichment over pre-bomb ^{14}C levels (i.e., a small amplitude
581 change in $\Delta^{14}C$ values) is generally observed during the peak in ^{14}C activity. This delayed
582 response implies that some portion of these fatty acids were recently synthesized and
583 deposited (within one or two decades) in Cariaco sediments, whereas there are no
584 significant contributions from a more instantaneously (e.g., seasonally or annually)
585 delivered component. This "decadal" signature is superimposed on an additional plant wax
586 pool that is substantially older. These preliminary interpretations appear consistent with a
587 relatively rapid supply of recently synthesized vascular plant carbon (illustrated by a swift
588 response of the leaf wax $\Delta^{14}C$ to bomb-spike enrichment), accompanied by an older [soil]
589 signature from the small watersheds of the two main rivers (Unare and Tuy) that discharge
590 in close proximity to the Cariaco Basin. While eolian transport can deliver terrestrial
591 organic matter on short timescales, this input is considered improbable because the
592 prevailing northeast trade winds establish a persistent onshore or alongshore flow in this
593 region.

594 In contrast, the distinct, albeit subtle, ^{14}C enrichment in the long-chain fatty acids
595 from Saanich Inlet (measured as the combined $nC_{26+28+30+32}$ homologues; Fig. 6a) is coeval
596 with the peak in atmospheric bomb $\Delta^{14}CO_2$. Unlike the Cariaco Basin, prevailing winds
597 and the inland setting of Saanich may allow rapid eolian delivery of some fraction of the
598 leaf wax flux, however direct runoff from the heavily vegetated and steeply sloping

599 hillsides surrounding the inlet seems more likely. The generally lower $\Delta^{14}C$ values and
600 lower amplitude enrichment over pre-bomb values in the Saanich record, however, imply
601 the presence of a larger and/or more extensively aged plant wax component, presumably
602 derived from protracted storage in an intermediate reservoir such as soils.

603 The composite long-chain fatty acid ($nC_{24+26+28+30}$) $\Delta^{14}C$ values for the Mackenzie
604 Delta show a clear maximum around 1968 (in contrast with the $\Delta^{14}C_{TOC}$ peak in 1975),
605 which is in between the initial responses found in the Saanich Inlet (1964) and Cariaco
606 Basin (1975) cores, and could be indicative of a relatively responsive pool of OC (Fig. 6a).
607 The onset of bomb-spike enrichment appears relatively early, however, indicating a greater
608 contribution from an "annual" pool than for the other two locations. A second, lower
609 amplitude peak is also evident in the mid/late 1990s, possibly indicating OC release from
610 an intermediate reservoir. Apart from these two peaks, we observe a slowly decreasing
611 composite $\Delta^{14}C$ value of $nC_{24+26+28+30}$ from 1890 to 1950, pointing towards a gradual but
612 consistent aging during this period of more than 50‰. This trend may continue during the
613 rest of the 20th century, but is superimposed by other trends and not visible. The slow
614 increase in age is larger than would be expected based on the Suess effect alone (Levin and
615 Hesshaimer, 2000), and thus may reflect increased contributions of (permafrost) soil OC
616 of millennial age. This decreasing $\Delta^{14}C$ trend was corrected in the model by introducing a
617 linear term (see section 3.3).
618

619 **4.2. Constraining (soil) reservoir ages**

620 Constraining the age and fractional contribution of each source of lipid biomarkers
621 is beyond the scope of this study, because they likely integrate organic matter that
622 encounters and passes through a broad continuum of reservoirs ranging from those with
623 very short (such as the atmosphere) to potentially very long (soils and wetlands,
624 permafrost) residence times. Nonetheless, the relationship between the evolution in the
625 $\Delta^{14}C$ profiles of the fatty acid homologues and that of atmospheric CO_2 over the course of
626 the bomb-spike can be exploited in a modeling framework to quantitatively apportion their
627 sedimentary inventories into several temporally distinct components. Based on the above
628 (section 2.6), these components are initially defined as contributions from vascular plant
629 material delivered to sediments (*i*) from annual to decadal reservoirs after the bomb-spike

630 (defined as the 'young' pool; younger than ca. 50 years), and (*ii*) from centennial to
631 millennial reservoirs prior to the bomb-spike (defined as the 'old' pool; older than 50 years).
632 This apportionment is broadly analogous to ^{14}C-based modeling studies of soil C turnover
633 (e.g., Harrison, 1996; Tegen and Dörr, 1996; Mills et al., 2013). Because we consider the
634 vascular plant-derived (>*n*C_{24} long-chain *n*-alkanoic acids) material indicative solely of the
635 terrigenous contribution to the sediments, we have not incorporated contributions from
636 marine material.

637 The model results show that the contribution of old leaf wax material to the
638 sediments in our systems is quite substantial, from 49-52% for the Saanich Inlet and
639 Mackenzie Delta, to 64-78% in the Cariaco Basin, depending on the modeling results of
640 $C_{26\text{-}28\text{-}30\text{-}32}$ and $C_{30\text{-}32}$ chains for the latter location, respectively (Fig. 7 and Table 2). Note,
641 however, that the modelled (calendar) age of old material (τ_{Old}) for these different systems
642 is rather variable (Table 2), from relatively young in Cariaco (both sets of chain-lengths
643 analyzed; 2400-3200 years), to intermediate old ages at Saanich Inlet (close to 7900 years)
644 to significantly older material in Mackenzie (28,000 years; Fig. 3C and Table 1). However,
645 the absolute values of τ_{Old} should be interpreted with care and viewed as approximations
646 also because our model works with the assumption that source proportions (and hence their
647 mean age) are constant which is not accurate. The variable results for the two different
648 modeling exercises of Cariaco Basin fatty acids ($C_{26\text{-}28\text{-}30\text{-}32}$ and $C_{30\text{-}32}$ chains) indicate that
649 longer chain lengths exhibit, on average, longer residence times in the system, potentially
650 reflecting their relatively recalcitrant nature. This finding touches upon the age-reactivity
651 distribution in organic matter in general, that may be further investigated using different
652 techniques such as ramped pyrolysis ^{14}C analysis (e.g. Rosenheim and Galy, 2012).

653 Looking at the detailed modeled profiles for residence times less than 50 years (Fig.
654 8; Table 2; Fig. S4), the younger, more dynamic fatty acid pool in the Mackenzie Delta is
655 dominated by an instantaneous/annual contribution (0-2 years; 24%) and a decadal
656 contribution of 15-35 year old material. Saanich Inlet also shows a distinct annual
657 contribution (0-2 years; 16% of young pool), while Cariaco Basin shows a relatively high
658 contribution of material between 5 and 10 years old (24% of young pool, Fig. 8; Table 2).
659 For Cariaco Basin and Saanich Inlet, the proportion of leaf wax derived acids approaches

660 the estimated contribution for residence times of 30 years and higher, which is a
661 consequence of low data resolution deeper in the sediment cores.
662 A recent study by French et al. (2018) used a different, yet broadly comparable,
663 two-component isotope-mixing model combined with modeling of a fast- and slow-cycling
664 component on downcore fatty acid $\Delta^{14}C$ data from a core collected in the Bay of Bengal
665 that receives material from the Ganges-Brahmaputra watershed. They find that 79 to 83%
666 of the fatty acids in this core have resided for 1000 to 1200 years in the catchment, while
667 the remainder was stored for an average of 15 years. We tested running their data with our
668 model to test if results where comparable. We found that 73±2% of the fatty acids were
669 stored for 1330±76 years when modeling the composite $\Delta^{14}C$ value of $nC_{24+26+28+30+32}$ while
670 75±4% of the fatty acids were stored for about 1310±150 years (Table S4) when modeling
671 only the nC_{28} homologue and treating 1975 as an outlier. French et al. (2018) did not
672 incorporate any linear term to correct for trends observed prior to the bomb-spike (our
673 parameter b), as their core started in 1945. For that reason, we also set parameter b to 0.
674 These results show that our model is capable of predicting the age and residence time of
675 fatty acid components across a wider range of catchments than the three included in this
676 work.
677
678 **4.3. Analysis and Implications**
679 The residence time of vascular plant OC in continental drainage basins may be
680 expected to vary as a function of intrinsic physicochemical properties such as structure,
681 size, polarity, reactivity and mineral association, as well as environmental and geomorphic
682 properties including temperature, permafrost, aridity, soil development, wind stress, and
683 the size and topographic relief of a particular catchment basin (Trumbore and Harden,
684 1997; Wang et al., 1999; Quideau et al., 2001). Moreover, anthropogenic activities such as
685 urbanization, damming, deforestation and cultivation of previously wooded landscapes in
686 the last few centuries have not only shifted the type of OC delivered to the aquatic
687 environment (Smittenberg et al., 2004; Wiesenberg et al., 2004), but have also altered its
688 rate of discharge as water flow patterns and/or structural integrity of soils are modified
689 (Wang et al., 1999; Smittenberg, 2003).

690 The observed variability within the younger (more responsive) pool of vascular
691 plant matter being delivered to our study sites (Fig. 8) can be explained by the factors
692 described above. The pronounced Spring freshet in the Mackenzie River generates a strong
693 flushing of surface soil and litter, delivering very recent material of 1-2 years old to the
694 fluvial network, as also supported by young DOC ages (Raymond et al., 2007). In contrast,
695 the distinct "annual" signal in the Saanich Inlet sediments most likely reflects rapid
696 transport from the steep, densely vegetated hillslopes in the nearby Cowichan River
697 catchment, strengthened by a high annual runoff of 2075 mm (Table 1). Cariaco Basin
698 sediments do not show a clear "annual" signal but instead indicate the presence of material
699 that is 5-10 years old. We hypothesize that this is annually-delivered terrestrial (fluvial)
700 matter influenced by transport time offshore, possibly mixed with minor contributions of
701 eolian inflow (Elmore et al., 2009, Martinez et al., 2010) and/or resuspended sediment from
702 the continental slope. A decadal signal (20-30 years) within the young pool is also observed
703 in the model results of the Mackenzie Delta, pointing to a pool of plant waxes that undergo
704 storage and/or transport on slightly longer timescales (Fig. 8). This delayed pattern may be
705 a consequence of cascading deposition and resuspension processes acting upon recent
706 Spring flood materials as sediments move through the delta. Alternatively, the decadal
707 signal may be the integrated signal of seasonal growth and runoff reflecting the annual
708 export from the large drainage basin (nearly 1.8 million km^2). The amount of precipitation
709 within these drainage basins may also play an important role, especially with respect to the
710 decadal pool. While more seasonal over northern South America than in coastal British
711 Columbia, annual mean rainfall is comparable between locales with ca. 750 and 900 mm,
712 respectively (Table 1). The large Mackenzie River watershed has on average a more
713 continental setting with an annual mean rainfall of 250-500 mm.
714 The disparity in the age of the old reservoirs in the Cariaco Basin, Saanich Inlet,
715 and Mackenzie watersheds indicates these respond to different properties of the drainage
716 basin. Potential factors include size and topographic relief of local rivers and their
717 associated watersheds, the age and development of the underlying soils, the
718 presence/absence of permafrost, floodplain dynamics, and annual and seasonal patterns of
719 temperature and precipitation. Differences in MAT for our catchments, ranging from -5°C
720 to 30°C (Table 1) may be the most obvious parameter explaining the order of magnitude

721 difference in old residence times. Currently, resolving other key controls is not possible in
722 the absence of similar molecular ^{14}C information for a broader range of fluvial systems.
723 Many previous investigations have uncovered evidence for annual to multi-millennial
724 residence times for lipids and bulk OC in soils (e.g., Harrison, 1996; Tegen and Dörr, 1996;
725 Rethemeyer et al., 2004; Smittenberg et al., 2006; Vonk et al., 2015; Hilton et al., 2015;
726 Van der Voort et al., 2017). Smittenberg et al. (2006) found that soil redevelopment
727 following glacial retreat in British Columbia was accompanied by a steady increase in the
728 age of higher plant alkanes accumulating in Saanich Inlet sediments over the Holocene.
729 The temporal resolution of that study (covering the past ca. 12,000 years) was far too coarse
730 to resolve a decadal component, but the reported ^{14}C-age of *n*-alkanes extracted from
731 surficial sediments (from 4800 to 7900 yrs BP; Smittenberg et al., 2004) reveals the
732 presence of ancient carbon reservoirs in this system that are similar in age to the residence
733 time for the old pool calculated here. Such close correspondence indicates that the age of
734 this reservoir may be linked to soil properties in a particular drainage basin, and predicts
735 that OC in soils surrounding the Saanich Inlet is more slowly cycled than that in northern
736 South America (Cariaco Basin). In the more northern Mackenzie Delta, recent studies
737 report the average ^{14}C-age of biogenic terrestrial OC (i.e. corrected for the simultaneously
738 released petrogenic component) delivered to the delta to be 5800 to 6100 years BP (Hilton
739 et al., 2015; Vonk et al., 2015). This is lower than the old residence time calculated here
740 (28 ky; Table 2), but these biogenic terrestrial OC ages are a composite of various pools of
741 organic compounds with different average residence times in the watershed, likely also
742 including a large fraction of younger compounds such as short-chain fatty acids, lignin or
743 hydroxy phenols that were measured to have approximate ages of 20, 2800, and 2900 years
744 BP in Mackenzie shelf sediments, respectively (Feng et al., 2015). An important factor for
745 the northern soils in this region is the presence of permafrost, which generally acts as a
746 delay for release of soil organic matter into fluvial systems, and increases the mean soil
747 OC residence time when the continuity of permafrost increases (Gustafsson et al., 2011).
748 However, the age of recalcitrant terrestrial compounds, such as plant wax lipids, tends to
749 be higher in regions of discontinuous permafrost, potentially due to increased hydrological
750 connectivity that affords OC mobilization from deeper soil horizons (Feng et al. 2013;
751 2015; Gustafsson et al., 2011). A large fraction of the Mackenzie watershed is underlain

752 by discontinuous permafrost, potentially explaining the modeled 28 ky for the residence
753 time of the old pool.

754 Lastly, it is important to point out that some portion of these residence times may
755 not be exclusively attributable to terrestrial reservoirs. Rather, vascular plant OC might
756 age significantly during repeated deposition/resuspension cycles in deltaic and inner shelf
757 sediments before ultimate burial in the lower energy regions of the continental margins
758 (Hedges and Keil, 1995; Bao et al., 2016). Although not expected to be a major effect in
759 the relatively small, steep-sided basin that comprises Saanich Inlet (turbidite deposits being
760 the notable exception) and perhaps only minor in the annually-flooded, but extensive
761 Mackenzie Delta, this effect might have a larger impact on ^{14}C ages of fatty acids in the
762 Cariaco Basin, where the mouths of the Tuy and Unare rivers are separated from the basin
763 by a relatively broad (up to ca. 50 km) shelf. Irrespective of the underlying processes
764 responsible for the translocation of terrestrial OC from its location of production to
765 receiving basin, it is clear that resulting sedimentary signatures incorporate convoluted
766 storage and transport histories that must be considered in carbon cycle studies and in
767 interpretation of sedimentary records.
768
769 **5. CONCLUSION**

770 Compound-specific radiocarbon analysis of long-chain fatty acids isolated from the
771 Cariaco Basin, Saanich Inlet, and Mackenzie Delta sediments indicates that a portion of
772 vascular plant OC is aged for several millennia on the continents prior to delivery to
773 adjacent sedimentary deposits. Comparison of down-core $\Delta^{14}C$ profiles of fatty acids to
774 $\Delta^{14}C$ variations in atmospheric CO_2 over the 20^{th} century in a modeling framework
775 indicates that approximately 50 to >75% of the plant wax input was retained within the
776 watershed for several millennia, while the remainder experienced a much shorter delay of
777 only a few years to a few decades prior to export and deposition in the receiving basin.
778 Together with petrogenic debris, this old terrestrial material likely represents a primary
779 source of old OC currently being buried in deltaic and continental margin sediments.

780 The relative contributions of annual vs. decadal material in the young pool of our
781 catchments is likely determined by landscape-specific factors such as discharge, or
782 catchment relief. We reason that the strikingly different ages of the millennially-aged old

carbon pool at our study sites (ranging between 2.4 and 28 ky old) may be driven by larger-scale climatic factors such as MAT. As our catchments cover about 60 degrees of latitude, the MAT values vary from +30ºC to -5 ºC, which may be an important driver for these age contrasts, as MAT drives e.g. rates of soil formation, OC turnover, and stability (e.g., permafrost), which may in turn impact the vascular plant OC residence times in terrestrial systems.

While we should not neglect the limitations of our modeling approach, it seems that our model is sufficiently robust to predict comparable age and residence time of terrestrial OC from the Ganges-Brahmaputra watershed that was recently modeled by French et al. (2018). Pre-aging of vascular plant OC in terrestrial reservoirs prior to sedimentary accumulation may have important implications for the interpretation of paleoclimate records based on vascular plant biomarkers and their temporal relationships to other proxies of marine and terrestrial conditions. Down-core variations in the distributions and $\delta^{13}C$ and δD compositions of leaf waxes are being increasingly employed to reconstruct fluctuations in continental aridity (Meyers, 1997; Hughen et al., 2004; Makou et al., 2007; Giosan et al., 2017; Schefuss et al., 2003). Although decadal residence times alone would have a minimal impact on the interpretation of these records, supply of extensively aged biomarkers may result in phase-shifted or muted signals relative to marine and other terrestrial proxies, especially across rapid transitions in temperature and precipitation (e.g., Hughen et al., 2004). In general, any kind of paleoenvironmental material used in reconstructions (e.g. pollen, diatoms, charcoal) may be affected by this 'pre-aging' when prone to long-term storage and transport. Further research is therefore clearly needed to fully capture the extent and consequence of multi-millennial terrestrial residence times for any kind of fossil OC.

Acknowledgements. We thank Sheila Griffin for assistance with AMS target preparation, Carl Johnson for compound-specific $\delta^{13}C$ and elemental analysis expertise, Ana Lima for freeze core sampling guidance, NOSAMS for ^{14}C analysis and use of their PCGC facility, and the crews of the R/V *Clifford Barnes* and R/V *Hermano Gines* for their help in retrieving sediment cores from the Saanich Inlet and Cariaco Basin, respectively. For Mackenzie sediment core sampling we wish to thank William Hurst, Tommy Smith,

Dennis Felix and the Aurora Research Institute, the Inuvialuit Land Administration and the Gwich'in Renewable Resource Board, as well as Valier Galy, Sarah Brody, David Griffith, Marshall Moore, Skye Moret, Michaelene Nelson, Camilo Ponton, and Rebecca Sorrell. Financial support was provided by a Schlanger Ocean Drilling Graduate Fellowship (NJD), an EPA STAR Graduate Fellowship (NJD), a Dutch NWO Veni grant #825.10.022 (JEV), US NSF grants #OCE-0137005 (TIE and KAH), #OCE-052626800 (TIE), #OCE-0961980 (ERMD), and #EAR-0447323 (ERMD and JRS), a Swiss SNF grant #200021_140850 (TIE), a Swedish Research Council grant #2013-05204 (MS), as well as the Stanley Watson Chair for Excellence in Oceanography at WHOI (TIE) and the WHOI Arctic Research Initiative (TIE and LG).

REFERENCES

Anderson J.J. and Devol A.H. (1973) Deep water renewal in Saanich Inlet, an intermittently anoxic basin. *Estuarine and Coastal Mar. Sci.* **1**, 1-10.

Astor Y., Muller-Karger F. and Scranton M.I. (2003) Seasonal and interannual variation in the hydrography of the Cariaco Basin: Implications for basin ventilation. *Cont. Shelf Res.* **23**, 125-144.

Bao R., McIntyre C., Zhao M., Zhu C., Kao S.-J. and Eglinton T.I. (2016) Widespread dispersal and aging of organic carbon in shallow marginal seas. *Geology* **44**, 791-794.

Berner R.A. (1989) Biogeochemical cycles of carbon and sulfur and their effect on atmospheric oxygen over Phanerozoic time. *Palaeogeogr. Palaeocl.* **73**, 97-122.

Blais-Stevens A., Clague J.J., Bobrowsky P.T. and Patterson R.T. (1997) Late Holocene sedimentation in Saanich Inlet, British Columbia, and its paleoseismic implications. *Canadian J. Earth Sci*. **34**, 1345-1357.

Bonell M., Hufschmidt M.M. and Gladwell J.S. (1993) Hydrology and water management in the humid tropics. Cambridge University Press, Cambridge, UK.

Bröder L., Tesi T., Anderson A., Semiletov I. and Gustafsson Ö. Bounding cross-shelf transport time and degradation in Siberian-Arctic land-ocean carbon transfer, accepted in Nature Communications.

Canuel E.A. and Martens C.S. (1996) Reactivity of recently deposited organic matter: Degradation of lipid compounds near the sediment-water interface. *Geochim. Cosmochim. Acta* **60**, 1793-1806.

Carson M.A., Jasper J.N. and Conly F.M. (1998) Magnitude and sources of sediment input to the Mackenzie Delta, Northwest Territories, 1974–94. *Arctic* **51**, 116–124.

Chikaraishi Y. and Naraoka H. (2006) Carbon and hydrogen isotope variation of plant biomarkers in a plant-soil system. *Chem. Geol.* **231**, 190-202.

Clark J.S. and Gelfand A.E. (2006) Hierarchical modelling for the Environmental Sciences: Statistical methods and applications. Oxford University Press on Demand.

Collister J.W., Rieley G., Stern, B., Eglinton G. and Fry B. (1994) Compound-specific $\delta^{13}C$ analyses of leaf lipids from plants with differing carbon dioxide metabolisms. *Org. Geochem.* **21**, 619-627.

Conte M.H. and Weber J.C. (2002) Plant biomarkers in aerosols record isotopic discrimination of terrestrial photosynthesis. *Nature* **417**, 639-641.

Cowie G.L., Hedges J.I. and Calvert S.E. (1992) Sources and reactivities of amino acids, neutral sugars, and lignin in an intermittently anoxic marine environment. *Geochim. Cosmochim. Acta* **56**, 1963-1978.

Crowley T.J. (1995) Ice age terrestrial carbon changes revisited. *Global Biogeochem. Cycles* **9**, 377-389.

Dean J.M. and Kemp A.E.S. (2004) A 2100 year BP record of the Pacific Decadal Oscillation, El Niño Southern Oscillation and Quasi-Biennial Oscillation in marine production and fluvial input from Saanich Inlet, British Columbia. *Palaeogeo., Palaeoclim., Palaeoecol.* **213**, 207-229.

Doney S.C., Lindsay K., Caldeira K., Campin, J.-M., Drange J., Dutay J.-C., Follows M., Gao Y., Gnanadesikan A., Gruber N., Ishida A., Joos F., Madec G., Maier-Reimer E., Marshall J.C., Matear R.J., Monfray P., Mouchet A., Najjar R., Orr J.-C., Plattner G.-K., Sarmiento J., Schlitzer R., Slater R., Totterdell I.J., Weirig M.-F.,

Yamanaka Y. and Yool A. (2004) Evaluating global ocean carbon models: The importance of realistic physics. *Global Biogeochem. Cycles* **18**, doi:10.1029/2003GB002150.

Drenzek N.J., Hughen K.A., Montluçon D.B., Southon J.R., dos Santos G.M., Druffel E.R.M., Giosan L. and Eglinton T.I. (2009). A new look at old carbon in active margin sediments. *Geology* **37**, 239-242.

Drenzek N.J., Montluçon D.B., Yunker M.B., Macdonald R.W. and Eglinton T.I. (2007). Constraints on the origin of sedimentary organic carbon in the Beaufort Sea from coupled ^{13}C and ^{14}C measurements. *Mar. Chem.* **103**, 146-162.

Drenzek N.J. (2007) The temporal dynamics of terrestrial organic matter transfer to the oceans: initial assessment and application. PhD thesis, Woods Hole Oceanographic Institution, Massachusettes Institute of Technology, Boston, US.

Druffel E.R.M. (1983) Long-term variability of temperature and carbon-14 in the Gulf Stream: Oceanographic implications. *Radiocarbon* **25**, 449-458.

Druffel E.R.M. (1987) Bomb radiocarbon in the Pacific: Annual and seasonal timescale variations. *J. Mar. Res.* **45**, 667-698.

Druffel E.R.M. (1996) Post-bomb radiocarbon records of surface corals from the tropical Atlantic Ocean. *Radiocarbon* **38**, 563-572.

Eglinton G. and Hamilton R.J. (1967) Leaf epicuticular waxes. *Science* **156**, 1322-1335.

Eglinton T.I., Aluwihare L.I., Bauer J.E. and Druffel E.R.M. (1996) Gas chromatographic isolation of individual compounds from complex matrices for radiocarbon dating. *Anal. Chem.* **68**, 904-912.

Eglinton T.I., Benitez-Nelson B.C., Pearson A., McNichol A.P., Bauer J.E. and Druffel E.R.M. (1997) Variability in radiocarbon ages of individual organic compounds from marine sediments. *Science* **277**, 796-799.

Elmore, A. C., Thunell, R. C., Styles, R., Black, D., Murray, R. W., Martinez, N. and Astor, Y. (2009) Quantifying the seasonal variations in fluvial and eolian sources of terrigenous material to Cariaco Basin, Venezuela. *J. S. Am. Earth Sci.* **27**, 197-210.

Emmerton C.A., Lesack L.F.W. and Marsh P. (2007) Lake abundance, potential water storage, and habitat distribution in the Mackenzie River Delta, western Canadian Arctic. *Water Resour. Res*. **43**, W05419.

Feng X., Gustafsson, Ö., Holmes, R. M., van Dongen, B. E., Semiletov, I. P., Dudarev, O. V., Yunker, M. B., Macdonald, R. W., Wacker, L., Montlucon, D. B. and Eglinton, T. I. (2015) Multimolecular tracers of terrestrial carbon transfer across the pan-Arctic: ^{14}C characteristics of sedimentary carbon components and their environmental controls, Global Biogeochem. Cyclues 29, 1855-1873, doi:10.1002/2015GB005204.

Feng X., Vonk, J. E., van Dongen, B. E., Gustafsson, Ö., Semiletov, I. P., Dudarev, O. V., Wang, Z., Montlucon, D. B., Wacker, L. and Eglinton, T. I. (2013) Differential mobilization of terrestrial carbon pools in Eurasian Arctic river basins, *P. Natal. Acad. Sci. USA* **110**, 14168-14173.

French K. L., Hein C. J., Haghipour N., Wacker L., Kudrass H. R., Eglinton T. I. and Galy V. (2018) Millennial soil retention of terrestrial organic matter deposited in the Bengal Fan, *Scientific Reports* **8**:11997, doi:10.1038/s41598-018-30091-8

Gagosian R.B. and Peltzer E.T. (1986) The importance of atmospheric input of terrestrial organic material to deep sea sediments. *Org. Geochem.* **10**, 661-669.

Galy V. and Eglinton T.I. (2011) Protracted storage of biospheric carbon in the Ganges-Brahmaputra basin. *Nature Geoscience* **4**, 843-847.

Galy V., Beyssac, O., France-Lanord, C. Eglinton, T. (2008) Recycling of graphite during Himalayan erosion: A geological stabilization of carbon in the crust. *Science*, **322**, 943-945, DOI: 10.1126/science.1161408.

Galy V., France-Lanord C., Beyssac O., Faure P., Kudrass H. and Palhol F. (2007) Efficient organic carbon burial in the Bengal fan sustained by the Himalayan erosional system. *Nature*, **450**: 407-410.

Giosan L., Ponton C., Usman M., Blusztajn J., Fuller D.Q., Galy V., Haghipour N., Johnson J.E., McIntyre C., Wacker L. and Eglinton T.I. (2017) Massive erosion in monsoonal central India linked to late Holocene landcover degradation. *Earth Surf. Dynam*. **5**, 781-789.

Gong C. and Hollander D.J. (1997) Differential contribution of bacteria to sedimentary organic matter in oxic and anoxic environments, Santa Monica Basin, California. *Org. Geochem.* **26**, 545-563.

Goñi M.A., Yunker M.B., Macdonald W.R. and Eglinton T.I. (2005) The supply and preservation of ancient and modern components of organic carbon in the Canadian Beaufort Shelf of the Arctic Ocean. *Mar. Chem.* **93**, 53-73.

Griffith D.R., Martin W.R. and Eglinton T.I. (2010) The radiocarbon age of organic carbon in marine surface sediments. *Geochim. Cosmochim. Acta.* **74**, 6788-6800.

Gucluer S.M. and Gross M.G. (1964) Recent marine sediments in Saanich Inlet, a stagnant marine basin. *Limnol. Oceanog.* **9**, 359-376.

Guilderson T.P., Cole J.E. and Southon J.R. (2005) Pre-bomb $\Delta^{14}C$ variability and the Suess effect in Cariaco Basin surface waters as recorded in hermatypic corals. *Radiocarbon* **47**, 57-65.

Gustafsson Ö., van Dongen B. E., Vonk J. E., Dudarev O. V. and Semiletov I. P. (2011) Widespread release of old carbon across the Siberian Arctic echoed by its large rivers, *Biogeosciences* **8**, 1737-1743.

Hamilton S.E. and Hedges J.I. (1988) The comparative geochemistries of lignins and carbohydrates in an anoxic fjord. *Geochim. Cosmochim. Acta* **52**, 129-142.

Harrison K.G. (1996) Using bulk soil radiocarbon measurements to estimate soil organic matter turnover times: Implications for atmospheric CO_2 levels. *Radiocarbon* **38**, 181-190.

Hedges J. I. and Keil R.G. (1995) Sedimentary organic matter preservation: an assessment and speculative synthesis, *Mar. Chem.* **49**, 81-115.

Hedges J.I. and Oades J.M. (1997) Comparative organic geochemistries of soils and marine sediments. *Org. Geochem.* **27**, 319-361.

Hedges J.I., Keil R.G. and Benner R. (1997) What happens to terrestrial organic matter in the ocean? *Org. Geochem.* **27**, 195-212.

Hijmans R.J., Cameron S.E., Parra J.L., Jones P.G. and Jarvis A. (2005). Very high resolution interpolated climate surfaces for global land areas. *International Journal of Climatology* **25**: 1965-1978.

Hilton R.G., Galy A., Hovius N., Horng M.J. and Chen H. (2011) Efficient transport of fossil organic carbon to the ocean by steep mountain rivers: An orogenic carbon sequestration mechanism. *Geology* **39**, 71-74.

965 Hilton R.G., Galy V., Gaillardet J., Dellinger M., Bruant C., O'Regan M., Gröcke D.R.,
966 Coxall H., Bouchez J. and Calmels D. (2015) Erosion of organic carbon in the
967 Arctic as a geological carbon dioxide sink. *Nature* **524**, 84-89.
968 Ho T.-Y., Taylor G.T., Astor Y., Varela R., Müller-Karger F. and Scranton M.I. (2004)
969 Vertical and temporal variability of redox zonation in the water column of the
970 Cariaco Basin: Implications for organic carbon oxidation pathways. *Mar. Chem.*
971 **86**, 89-104.
972 Holmes R.M., Coe M.T., Fiske G.J., Gurtovaya T., McClelland J.W., Shiklomanov A.I.,
973 Spencer R.G.M., Tank S.E. and Zhulidov A.V. (2013) Climate change impacts on
974 the hydrology and biogeochemistry of arctic rivers, In Climatic Change and Global
975 Warming of Inland Waters: Impacts and Mitigation for Ecosystems and Societies
976 (eds. C.R. Goldman, M. Kumagai and R.D. Robarts). John Wiley & Sons, Ltd, New
977 York
978 Hua Q. and Barbetti M. (2004) Review of tropospheric bomb ^{14}C data for carbon cycle
979 modeling and age calibration purposes. *Radiocarbon* **46**, 1273-1298.
980 Hua Q., Barbetti M. and Rakowski A.Z. (2013) Atmospheric radiocarbon for the period
981 1950–2010. *Radiocarbon* **55(4)**, 2059-2072.
982 Hughen K.A., Eglinton T.I., Xu L. and Makou M. (2004) Abrupt tropical vegetation
983 response to rapid climate change. *Science* **304**, 1955-1959.
984 Hughen K.A., Overpeck J.T., Peterson L.C. and Anderson R.F. (1996) The nature of varved
985 sedimentation in the Cariaco Basin, Venezuela, and its paleoclimate significance.
986 In *Palaeoclimatology and Palaeoceanography from Laminated Sediments* (ed.
987 A.E.S. Kemp). Geol. Soc. London, London. pp. 171-183.
988 Hwang J. and Druffel E.R.M. (2003) Lipid-like material as the source of the
989 uncharacterized organic carbon in the ocean? *Science* **299**, 881-884.
990 Keil R.G., Mayer L.M., Quay P.D., Richey J.E. and Hedges J.I. (1997) Loss of organic
991 matter from riverine particles in deltas. *Geochim. Cosmochim. Acta* **61**, 1507-1511.
992 Keil R.G., Tsamakis E., Fuh C.B., Giddings J.C. and Hedges J.I. (1994) Mineralogical and
993 textural controls on the organic composition of coastal marine sediments:
994 Hydrodynamic separation using SPLITT-fractionation. *Geochim. Cosmochim. Acta*
995 **56**, 879-893.
996 Klaminder J., Appleby P., Crook P. and Renberg I. (2012) Post-depositional diffusion of
997 137Cs in lake sediment: Implications for radiocaesium dating. *Sedimentology* **59**,
998 2259-2267.
999 Kunst L. and Samuels A.L. (2003) Biosynthesis and secretion of plant cuticular wax. *Prog.*
1000 *Lipid Res.* **42**, 51-80.
1001 Levin I. and Kromer B. (2004) The tropospheric $^{14}CO_2$ level in mid-latitudes of the
1002 northern hemisphere (1959-2003). *Radiocarbon* **46**, 1261-1272.
1003 Levin, I. and Hesshaimer V. (2000) Radiocarbon - a unique tracer of global carbon cycle
1004 dynamics. *Radiocarbon* **42**, 69-80.
1005 Lichtfouse É. (1999) Temporal pools of individual organic substances in soil. *Analysis* **27**,
1006 442-444.
1007 Lorenzoni L. (2005) The influence of local rivers on the eastern Cariaco Basin, Venezuela.
1008 MS Thesis. University of South Florida, 778 p.

1009 Makou M.C., Hughen K.A., Xu L., Sylva S.P. and Eglinton T.I. (2007) Isotopic records of
1010 tropical vegetation and climate change from terrestrial vascular plant biomarkers
1011 preserved in Cariaco Basin sediments. *Org. Geochem.* **38**, 1680-1691.
1012 Martin E.E., Ingalls A.E., Richey J.E., Keil R.G., Santos G.M., Truxal L.T., Alin S.R. and
1013 Druffel E.R.M. (2013) Age of riverine carbon suggests rapid export of terrestrial
1014 primary production in tropics. *Geophys. Res. Lett.* **40**, 5687-5691.
1015 Martinez N.C., Murray R.W., Thunell R.C., Peterson L.C., Muller-Karger F., Lorenzoni L.,
1016 Astor Y. and Varela R. (2010) Local and regional geochemical signatures of surface
1017 sediments from the Cariaco Basin and Orinoco Delta, Venezuela. *Geology* **38**, 159-
1018 162.
1019 Martinez, N. C., Murray, R.W., Thunell, R.C., Peterson, L.C., Muller-Karger, F.E., Astor,
1020 Y. and Varela, R. (2007) Modern climate forcing of terrigenous deposition in the
1021 tropics (Cariaco Basin, Venezuela). *Earth Planet Res. Lett*. **264**, 438-451.
1022 Matsumoto K., Kawamura K., Uchida M., Shibata Y. and Yoneda M. (2001) Compound-
1023 specific radiocarbon and $\delta^{13}C$ measurements of fatty acids in a continental aerosol
1024 sample. *Geophys. Res. Lett.* **28**, 4587-4590.
1025 Matsumoto K., Sarmiento J.L., Key R.M., Bullister J.L., Caldeira K., Campin J.-M., Doney
1026 S.C., Drange H., Dutay J.-C., Follows M., Gao Y., Gnanadesikan A., Gruber N.,
1027 Ishida A., Joos F., Lindsay K., Maier-Reimer E., Marshall J.C., Matear R.J.,
1028 Monfray P., Najjar R., Platter G.-K., Schlitzer R., Slater R., Swathi P.S., Totterdell
1029 I.J., Weirig M.-F., Yamanaka Y., Yool A. and Orr J.C. (2004) Evaluation of ocean
1030 carbon cycle models with data-based metrics. *Geophys. Res. Lett.* **31**, doi:
1031 10.1029/2003GL018970.
1032 McLean D., Galay V., Wright B. and Fleenor W. (2013) Integrating flood mitigations,
1033 sediment managemenet and habitat enhancement on coastal rivers of British
1034 Columbia, in: River Basin Management VII, WIT Transactions on Ecology and The
1035 Environment, Vol. 172, WIT Press.
1036 McQuoid M.R. and Hobson L.A. (1997) A 91-year record of seasonal and interannual
1037 variability of diatoms from laminated sediments in Saanich Inlet, British Columbia.
1038 *J. Plankton Res.* **19**, 173-194.
1039 Meyers P.A. (1997) Organic geochemical proxies of paleoceanographic, paleolimnologic,
1040 and paleoclimate processes. *Org. Geochem.* **27**, 213-250.
1041 Mills R.T.E., Tipping E., Bryant C.L. and Emmett B.A. (2013) Long-term organic carbon
1042 turnover rates in natural and semi-natural topsoils. *Biogeochemistry* **118**, 257-272,
1043 10.1007/s10533-013-9928-z.
1044 Nederbragt A.J. and Thurow J.W. (2001) A 6000 yr varve record of Holocene climate in
1045 Saanich Inlet, British Columbia, from digital sediment colour analysis of ODP Leg
1046 169S cores. *Mar. Geol.* **174**, 95-110.
1047 Ohkouchi N., Eglinton T.I. and Hayes J.M. (2003) Radiocarbon dating of individual fatty
1048 acids as a tool for refining Antarctic margin sediment chronologies. *Radiocarbon*
1049 **45**, 17-24.
1050 Pearson A. (1999) Biogeochemical applications of compound-specific radiocarbon
1051 analysis. Ph.D. thesis, MIT/WHOI Joint Program.
1052 Pearson A., McNichol A.P., Benitez-Nelson B.C., Hayes J.M. and Eglinton T.I. (2001)
1053 Origins of lipid biomarkers in Santa Monica Basin surface sediments: A case study

using compound-specific $\Delta^{14}C$ analysis. *Geochim. Cosmochim. Acta* **65**, 3123-3137.

Pearson A., McNichol A.P., Schneider R.J. and Von Reden K.F. (1998) Microscale AMS ^{14}C measurement at NOSAMS. *Radiocarbon* **40**, 61-75.

Pellatt M.G., Hebda R.J. and Mathewes R.W. (2001) High-resolution Holocene vegetation history and climate from hole 1034B, ODP leg 169S, Saanich Inlet, Canada. *Mar. Geol.* **174**, 211-226.

Price, A.M. and Pospelova, V. (2001) High-resolution sediment trap study of organic-walled dinoflagellate cyst production and biogenic silica flux in Saanich Inlet (BC, Canada). *Mar. Micropaleontol*. **80**, 18-43.

Quideau S.A., Chadwick O.A., Trumbore S.E., Johnson-Maynard J.L., Graham R.C. and Anderson M.A. (2001) Vegetation control on soil organic matter dynamics. *Org. Geochem.* **32**, 247-252.

Ratnayake N.P., Suzuki N. and Matsubara M. (2005) Sources of long chain fatty acids in deep sea sediments from the Bering Sea and the North Pacific Ocean. *Org. Geochem.* **36**, 531-541.

Raymond P.A., and Bauer J.E. (2001) Use of ^{14}C and ^{13}C natural abundances for evaluating riverine, estuarine, and coastal DOC and POC sources and cycling: A review and synthesis. *Org. Geochem.* **32**, 469-485.

Raymond P.A., McClelland J.W., Holmes R.M., Zhulidov A.V., Mull K., Peterson B.J., Striegl R.G., Aiken G.R. and Gurtovaya T.Y. (2007) Flux and age of dissolved organic carbon exported to the Arctic Ocean: A carbon isotopic study of the five largest arctic rivers. *Global Biogeochem. Cy.* **21**, GB4011.

Rethemeyer J., Kramer C., Gleixner G., Wiesenberg G.L.B., Schwark L., Andersen N., Nadeau M.-J. and Grootes P.M. (2004) Complexity of soil organic matter: AMS ^{14}C analysis of soil lipid fractions and individual compounds. *Radiocarbon* **46**, 465-473.

Rieley G., Collister R.J., Jones D.M. and Eglinton G. (1991) The biogeochemistry of Ellesmere Lake, U.K. – I: Source correlation of leaf wax inputs to the sedimentary lipid record. *Org. Geochem.* **17**, 901-912.

Robbins J.A., Holmes C., Halley R., Bothner M., Shinn E., Graney J., Keeler G., tenBrink M., Orlandini K.A. and Rudnick D. (2000) Time-averaged fluxes of lead and fallout radionuclides to sediments in Florida Bay, *J. Geophys. Res.* 105, C12, 28805-28821.

Rosenheim B.E., and Galy V. (2012) Direct measurement of riverine particulate organic carbon age structure. *Geophys. Res. Lett.* **39**, L19703,

Santos G.M., Moore R.B., Southon J.R., Griffin S., Hinger E. and Zhang D. (2007a) AMS ^{14}C sample preparation at the KCCAMS/UCI facility: Status report and performance of small samples. *Radiocarbon* **49**, 255-269.

Santos G.M., Southon J.R., Drenzek N.J., Ziolkowski L.A., Druffel E., Xu X., Zhang D., Trumbore S., Eglinton T.I. and Hughen K.A. (2010) Blank assessment for ultra-small samples: chemical extraction and separation vs. AMS. *Radiocarbon* **52**, 1322-1335.

Santos G.M., Southon J.R., Griffin S., Beaupre S.R. and Druffel E.R.M. (2007b) Ultra small-mass AMS ^{14}C sample preparation and analyses at KCCAMS/UCI facility. *Nucl. Inst. Methods Phys. Res. B* **259**, 308-315.

1100 Schefuss E., Ratmeyer V., Stuut J.-B.W., Jansen J.H.F. and Sinninghe Damste J.S. (2003)
1101 Carbon isotope analyses of n-alkanes in dust from the lower atmosphere over the
1102 central eastern Atlantic. *Geochim. Cosmochim. Acta* **67**, 1757-1767.
1103 Smittenberg R.H. (2003) Holocene environmental changes disclosed from anoxic fjord
1104 sediments by biomarkers and their radiocarbon content. Ph.D. thesis, University of
1105 Utrecht.
1106 Smittenberg R.H., Eglinton T.I., Schouten S. and Sinninghe Damsté J.S. (2006) Ongoing
1107 buildup of refractory organic carbon in boreal soils during the Holocene. *Science*
1108 **314**, 1283-1286.
1109 Smittenberg R.H., Hopmans E.C., Schouten S., Hayes J.M., Eglinton T.I. and Sinninghe
1110 Damsté J.S. (2004) Compound-specific radiocarbon dating of the varved Holocene
1111 sedimentary record of Saanich Inlet, Canada. *Paleoceanog.* **19,** doi:
1112 10.1029/2003PA000927.
1113 Tao S., Eglinton T.I., Montlucon D.B., McIntyre C.P. and Zhao M. (2015) Pre-aged soil
1114 organic carbon as a major component of the Yellow River suspended load: Regional
1115 significance and global relevance. *Earth Planet. Sci. Lett.* **414**, 77-86.
1116 Tao S., Eglinton T.I., Montlucon D.B., McIntyre C.P. and Zhao M. (2016) Diverse origins
1117 and pre-depositional histories of organic matter in contemporary Chinese marginal
1118 sea sediments. *Geochim. Cosmochim. Acta* **191**, 70-88.
1119 Tegen I. and Dörr H. (1996) ^{14}C measurements of soil organic matter, soil CO_2 and
1120 dissolved organic carbon (1987-1992). *Radiocarbon* **38**, 247-251.
1121 Thunell R.C., Varela R., Llano M., Collister J., Muller-Karger F. and Bohrer R. (2000)
1122 Organic carbon fluxes, degradation, and accumulation in an anoxic basin: Sediment
1123 trap results from the Cariaco Basin. *Limnol. Oceanog.* **45**, 300-308.
1124 Timothy D.A. and Soon M.Y.S. (2001) Primary production and deep-water oxygen content
1125 of two British Columbian fjords. *Mar. Chem.* **73**, 37-51.
1126 Timothy D.A., Soon M.Y.S. and Calvert S.E. (2003) Settling fluxes in Saanich and Jervis
1127 Inlets, British Columbia, Canada: Sources and seasonal patterns. *Prog. Oceanog*.
1128 **59**, 31-73.
1129 Trumbore S.E. and Harden J.W. (1997) Accumulation and turnover of carbon in organic
1130 and mineral soils of the BOREAS northern study area. *J. Geophys. Res. – Atm*. **102**,
1131 28817-28830.
1132 Tunnicliffe V. (2000) A fine-scale record of 130 years of organic carbon deposition in an
1133 anoxic fjord, Saanich Inlet, British Columbia. *Limnol. Oceanog*. **45**, 1380-1387.
1134 Uchida M., Shibata Y., Kawamura K., Kumamoto Y., Yoneda M., Ohkushi K., Harada N.,
1135 Hirota M., Mukai H., Tanaka A., Kusakabe M. and Morita M. (2001) Compound-
1136 specific radiocarbon ages of fatty acids in marine sediments from the western North
1137 Pacific. *Radiocarbon* **43**, 949-956.
1138 Van der Voort T.S., Zell C.I., Hagedorn F., Feng X., McIntyre C.P., Haghipour N., Graf
1139 Pannatier E. and Eglinton T.I. (2017) Diverse soil carbon dynamics expressed at
1140 the molecular level. *Geophys. Res. Lett.* **44**, 11840-11850.
1141 Vonk J. E., Dickens A. F., Giosan L., Hussain Z. A., Kim B., Zipper S. C., Holmes R. M.,
1142 Montlucon D. B., Galy V. and Eglinton T. I (2015) Arctic deltaic lake sediments as
1143 recorders of fluvial organic matter deposition, *Front. Earth Sci.* **4**:77,
1144 doi:10.3389/feart.2016.00077.

1145 Vonk J. E., Semiletov I. P., Dudarev O. V., Eglinton T. I., Andersson A., Shakhova N.,
1146 Charkin A., Heim B. and Gustafsson Ö. (2014) Preferential burial of permafrost-
1147 derived organic carbon in Siberian-Arctic shelf waters. *J. Geophys. Res. Oceans*
1148 **119**, doi:10.1002/2014JC010261.
1149 Vonk J.E., Giosan L., Blusztajn J., Montlucon D., Graf Pannatier E., McIntyre C., Wacker
1150 L., Macdonald R.W., Yunker M.B. and Eglinton T.I. (2015) Spatial variations in
1151 geochemical characteristics of the modern Mackenzie Delta sedimentary system.
1152 *Geochim. Cosmochim. Acta* **171**, 100-120.
1153 Wacker L., Fahrni S. M., Hajdas I., Molnar M., Synal H.-A., Szidat S. and Zhang Y. L.
1154 (2013) A versatile gas interface for routine radiocarbon analysis with a gas ion
1155 source. *Nucl. Instrum. Methods Phys. Res. B* **294**, 315–319.
1156 Walker B.D., Guilderson T.P., Okimura K.M., Peacock M.B. and McCarthy M.D. (2014)
1157 Radiocarbon signatures and size-age-composition relationships of major organic
1158 matter pools within a unique California upwelling system. *Geochim. Cosmochim.*
1159 *Ac*. **126**, 1-17.
1160 Wang Y., Amundson R. and Trumbore S. (1999) The impact of land use change on C
1161 turnover in soils. *Global Biogeochem. Cycles* **13**, 47-57.
1162 Weidman C.R. and Jones G.A. (1993) A shell-derived time history of bomb ^{14}C on Georges
1163 Bank and its Labrador Sea implications. *J. Geophys. Res.* **98**, 14577-14588.
1164 Wiesenberg G.L.B., Schwartzbauer J., Schmidt M.W.I. and Schwark L. (2004) Source and
1165 turnover of organic matter in agricultural soils derived from n-alkane/n-carboxylic
1166 acid compositions and C-isotope signatures. *Org. Geochem.* **35**, 1371-1393.
1167 Woo M.K. and Thorne R. (2003) Streamflow in the Mackenzie Basin, Canada. *Arctic* **56**,
1168 4, 328-340.
1169 Yarincik K.M., Murray R.W., Lyons T.W., Peterson L.C. and Haug G.H. (2000)
1170 Oxygenation history of bottom waters in the Cariaco Basin, Venezuela, over the
1171 past 578,000 years: Results from redox-sensitive metals (Mo, V, Mn, and Fe).
1172 *Paleoceanog*. **15**, 593-604.
1173 Yunker M.B., Backus S.M., Pannatier E.G., Jeffries D.S. and Macdonald R.W. (2002)
1174 Sources and significance of alkane and PAH hydrocarbons in Canadian Arctic
1175 rivers. *Estuarine and Coastal Mar. Sci.* **55**, 1-31.
1176
1177
1178
1179

TABLES

Table 1 - Sampling and watershed information for the Cariaco Basin, Saanich Inlet, and Mackenzie Delta

	Cariaco Basin	**Saanich Inlet**	**Mackenzie Delta**
Core IDs	CB2; CB5; CB6	SI3; SI4; SI7	MK07#6; MK09#2
Sampling location	10.500°N 64.670°W[a]	48.587°N 123.504°W[a]; 48.588°N 123.505°W; 48.590°N 123.504°W	68.672°N 134.566°W; 68.671°N 134.565°W
MAT (°C)[b]	30	10	-5
MAP (mm)[c]	ca. 800	ca. 900	250-500
Dominant vegetation	Tropical forest, plains, lowlands	Forest (conifers, cedars, oak)	Boreal forest (conifers), tundra, wetlands
Climate	Tropical	Moist maritime	Subarctic
Characteristics	Anoxic marine basin	Coastal fjord	Arctic delta
Dominant watershed	Unare River	Cowichan River	Mackenzie River
Watershed size (km^2)	3200[d]	800	1,750,000[h]
Discharge (km^3/year)	1.8[e]	1.66[g]	316[h]
Runoff (mm/year)[f]	560	2075	181[h]

a) Cariaco Basin: Three core barrels from one cast (multicorer-5, 305m water depth); Saanich Inlet: cores taken at 224m water depth.
b) Approximate Mean Annual Temperature (MAT) based in watersheds derived from ArcGIS World MAT map (Hijmans et al., 2005)
c) Mean Annual Precipitation (MAP) from www.climate-data.org
d) Data from www.es.wikipedia.org
e) Data from Bonell, Hufschmidt and Gladwell (1993).
f) Calculated from watershed size and discharge.
g) Data from Wateroffice Canada www.wateroffice.ec.gc.ca (station ID #08HA011, average 1960-2016)
h) Data from Holmes et al., 2013

Table 2: Estimated mean and standard deviations (between brackets) of the estimated predictive distributions of parameters b, f_{old}, and τ_{Old} as well as the fractional contributions (0-2 years, 0-5 years, 0-10 years, and 10-50 years). The young pool is operationally defined as <50 years, and all ages are reported in calendar years. Note that the young pool fractions consist of a total of 22-51% (1-f_{Old}), but are presented as a total contribution of 100%.

	Old pool contributions/age (y)		**Young pool contributions/age (y)**				
	f_{Old}	τ_{Old}	**0-2**	**0-5**	**0-10**	**10-50**	**b**
Mackenzie C24-26-28-30-32	0.52 (0.02)	28290 (9353)	0.24 (0.04)	0.32 (0.04)	0.42 (0.02)	0.58 (0.02)	-1.33 (0.13)
Saanich C26-28-30-32	0.49 (0.14)	7856 (5042)	0.16 (0.04)	0.18 (0.04)	0.28 (0.05)	0.72 (0.05)	-1.54 (0.53)
Cariaco C26-28-30-32	0.64 (0.1)	2382 (502)	0.04 (0.02)	0.08 (0.03)	0.32 (0.05)	0.68 (0.05)	-0.28 (0.28)
Cariaco C30+32	0.78 (0.07)	3174 (534)	0.08 (0.04)	0.13 (0.05)	0.30 (0.06)	0.70 (0.06)	0

FIGURES

Figure 1

Simplified schematic of potential transport pathways and intermediate storage reservoirs of terrestrial organic carbon (OC_{terr}) from biological source to marine sedimentary sink. Note that pre-aged OC (petrogenic or biospheric) also originates from atmospheric CO_2 and vascular plant OC but arrows are not shown here.

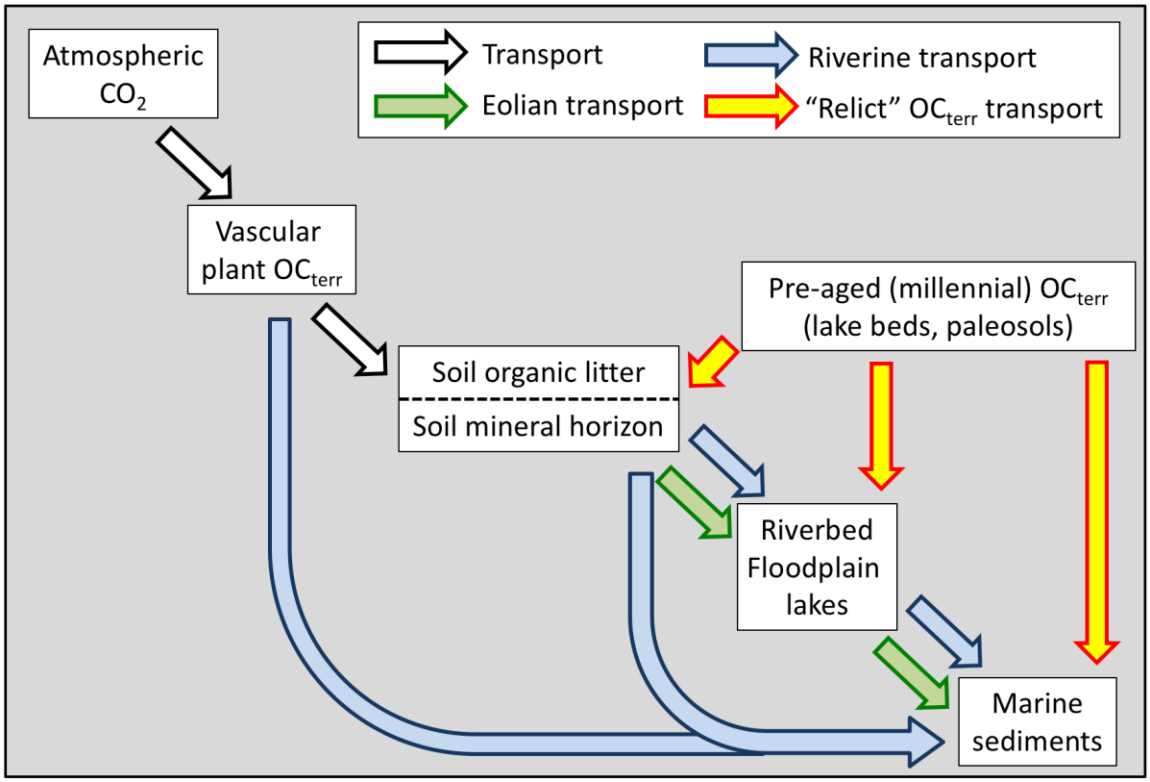

Figure 2

Maps of the (a) Cariaco Basin, (b) Saanich Inlet, and (c) Mackenzie Delta systems with major rivers, topography (contour lines at 500m interval), and coring sites (red) indicated, and (d) world map with locations indicated.

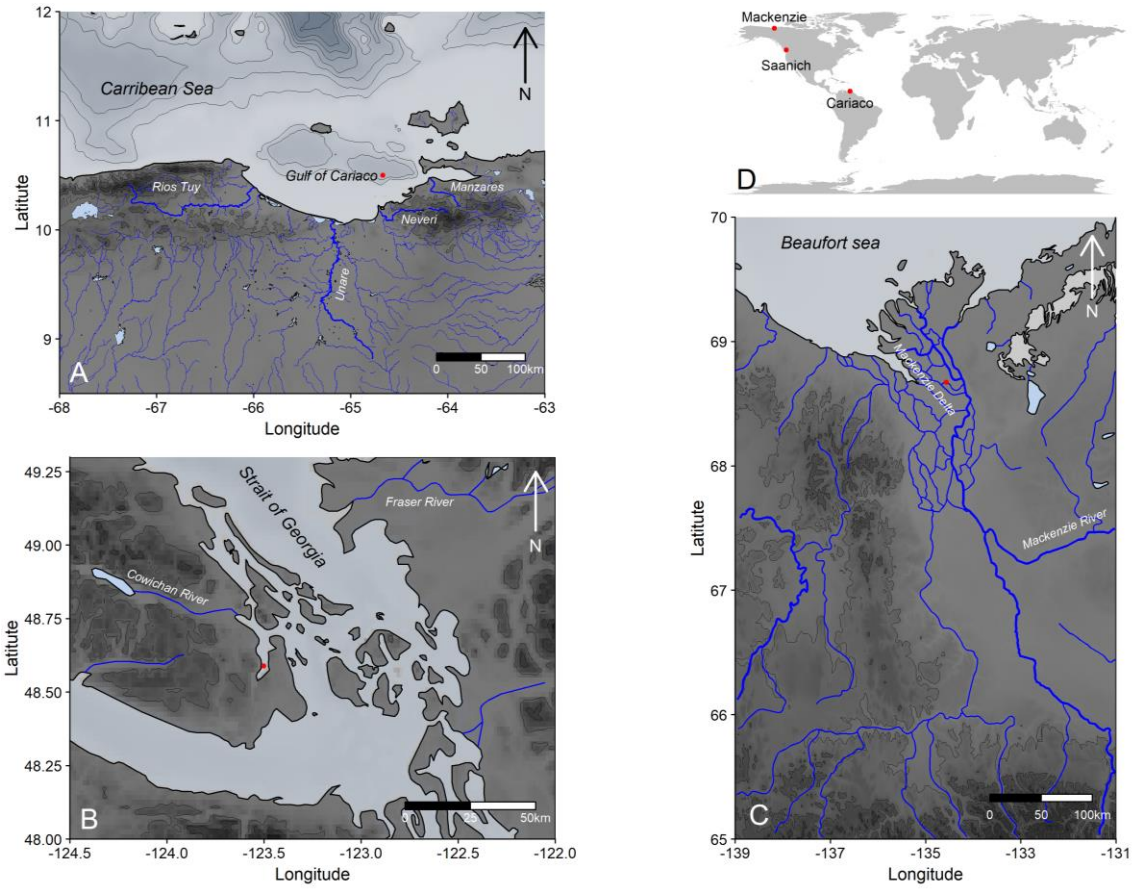

Figure 3

Chronology development for Cariaco Basin core #MC5 with (a) isotope activities of ^{210}Pb (green), ^{214}Pb (blue), and ^{137}Cs (red circles), and (b) plot of ln ^{210}Pb-xs against depth.

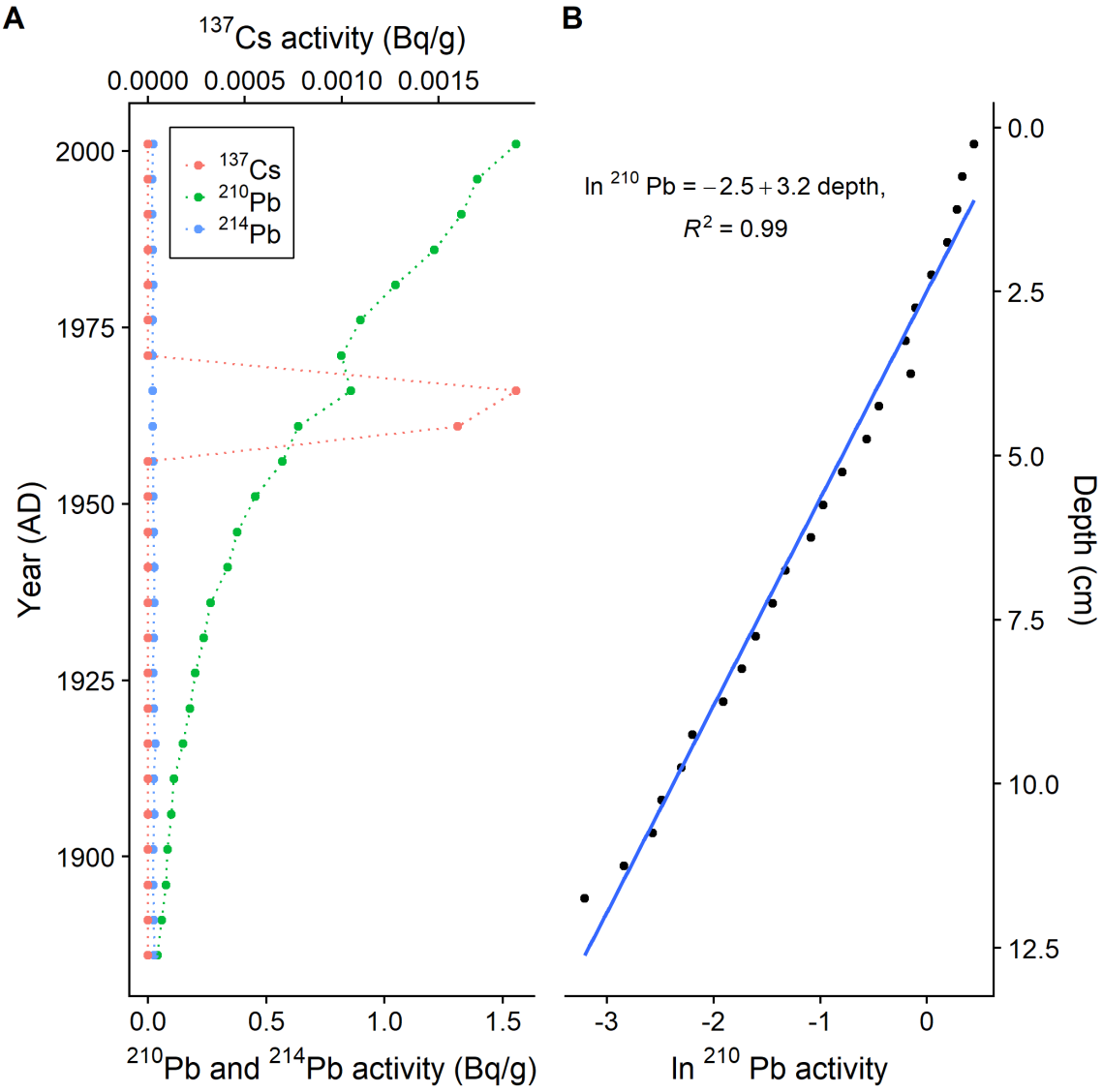

Figure 4

Chronology development for Saanich Inlet core #SI3 with (a) isotope activities of ^{210}Pb (green), ^{214}Pb (blue), and ^{137}Cs (red circles), and (b) plot of ln ^{210}Pb-xs against depth.

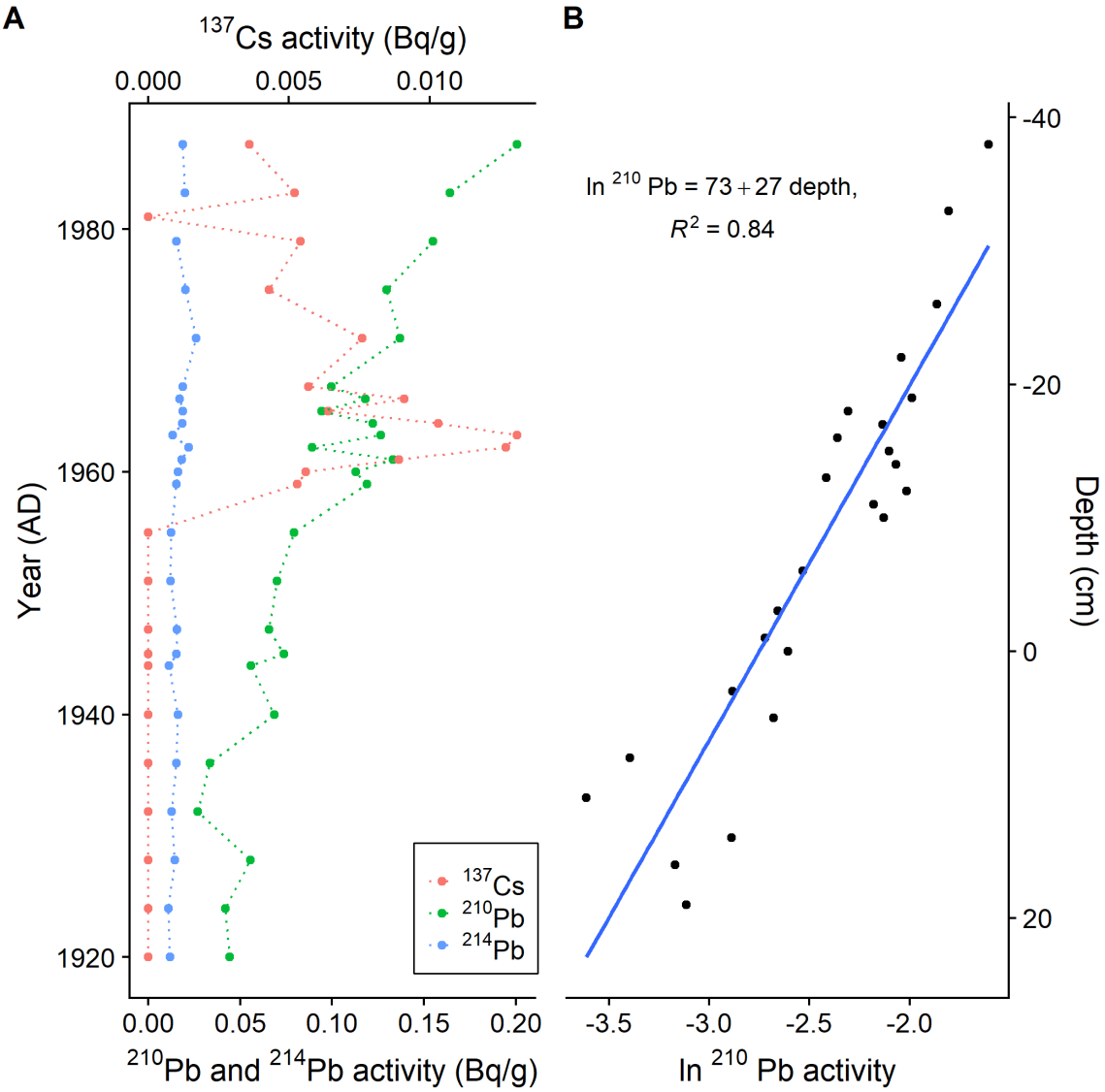

Figure 5

Chronology development for Mackenzie Delta lake core MK09#2 with isotope activity of ^{137}Cs, where the onset occurs at 60 cm depth (corresponding with 1951) and the peak at 52.5 cm depth (assuming to correspond to sedimentary deposition in 1964 from the atmospheric peak in 1963; Robbins et al., 2000, Klaminder et al., 2012).

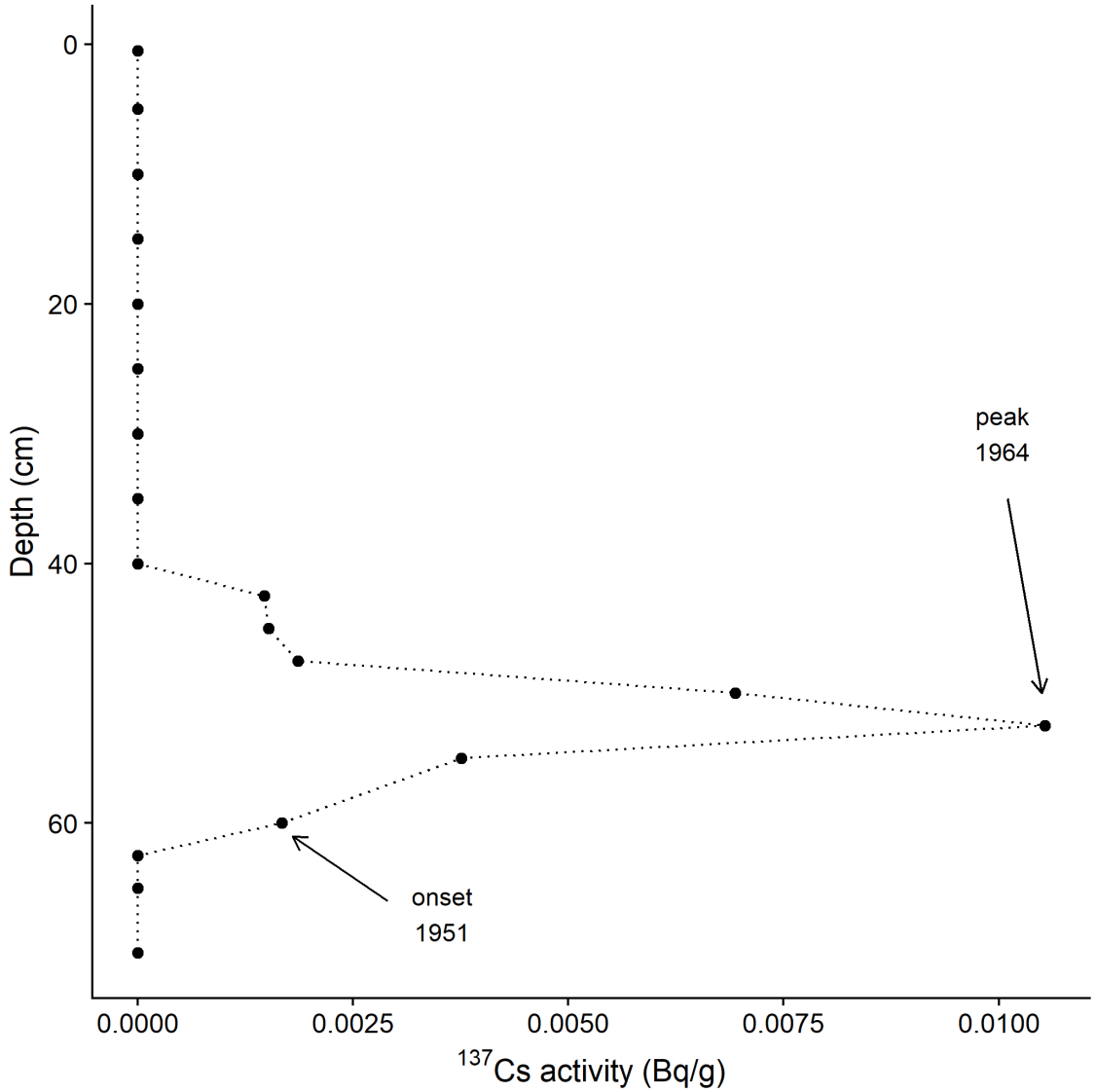

Figure 6

Fatty acid long-chain ^{14}C composition of (a) $nC_{26+28+30+32}$ combined for Cariaco Basin (red), Saanich Inlet (blue) and $nC_{24+26+28+30+32}$ combined for Mackenzie Delta (MK09#2; green circles), and individual long-chain *n*-alkanoic acids for (b) Saanich Inlet and (c) Cariaco Basin sediments. Note that in panel (a) the summed long-chain *n*-alkanoic acids are different from Mackenzie Delta ($nC_{24+26+28+30+32}$) than for the other locations ($nC_{26+28+30+32}$). The black dashed line represents the sedimentary deposition (1964) of the atmospheric bomb-spike signal in 1963.

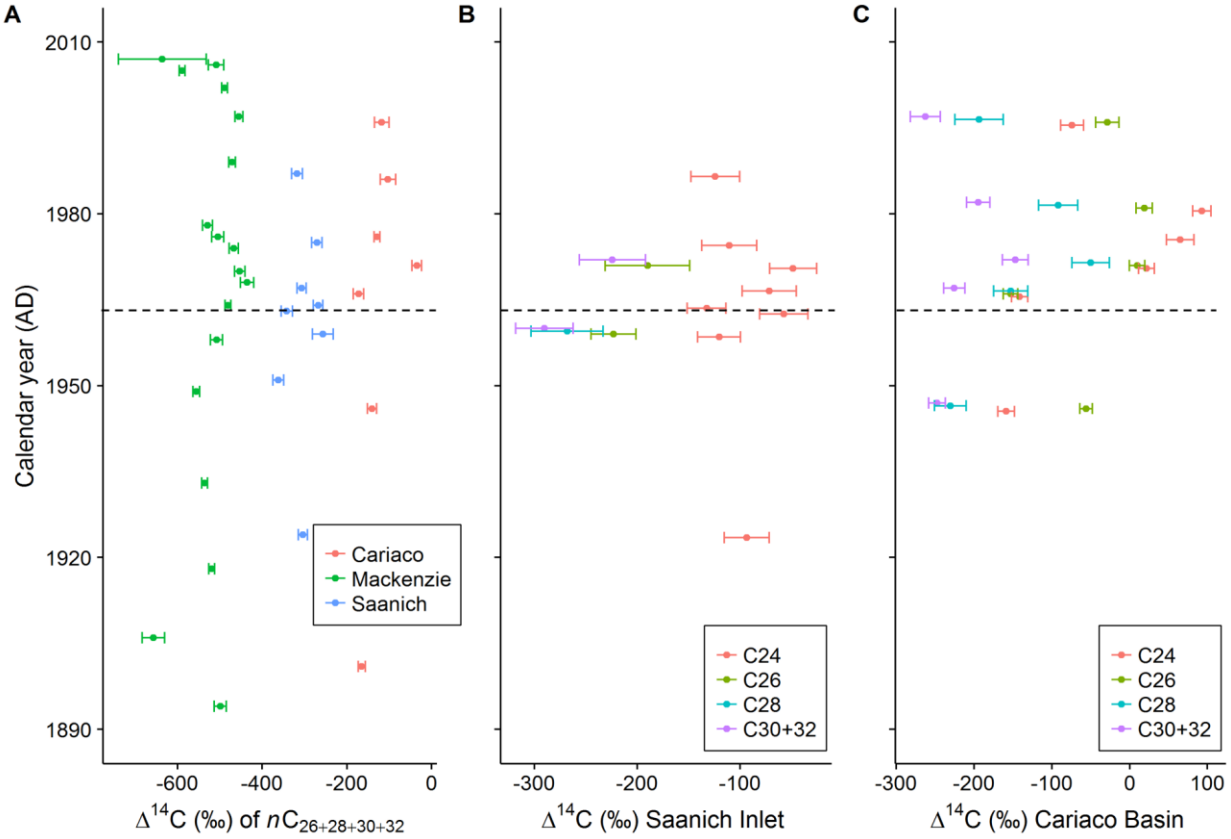

Figure 7

Model fits of estimated mean $\Delta^{14}C_{obs}(t)$ from equation [4] together with 90% credible interval and data, against calendar year in sediment cores, with (from left to right) Mackenzie Delta (light blue, $nC_{24+26+28+30+32}$), Saanich Inlet ($nC_{26+28+30+32}$), and Cariaco Basin (green, nC_{30+32} and red, $nC_{26+28+30+32}$). All data points are included in the model fit. Note that the nC_{30+32} model fit for Cariaco Basin is not corrected for the Suess effect.

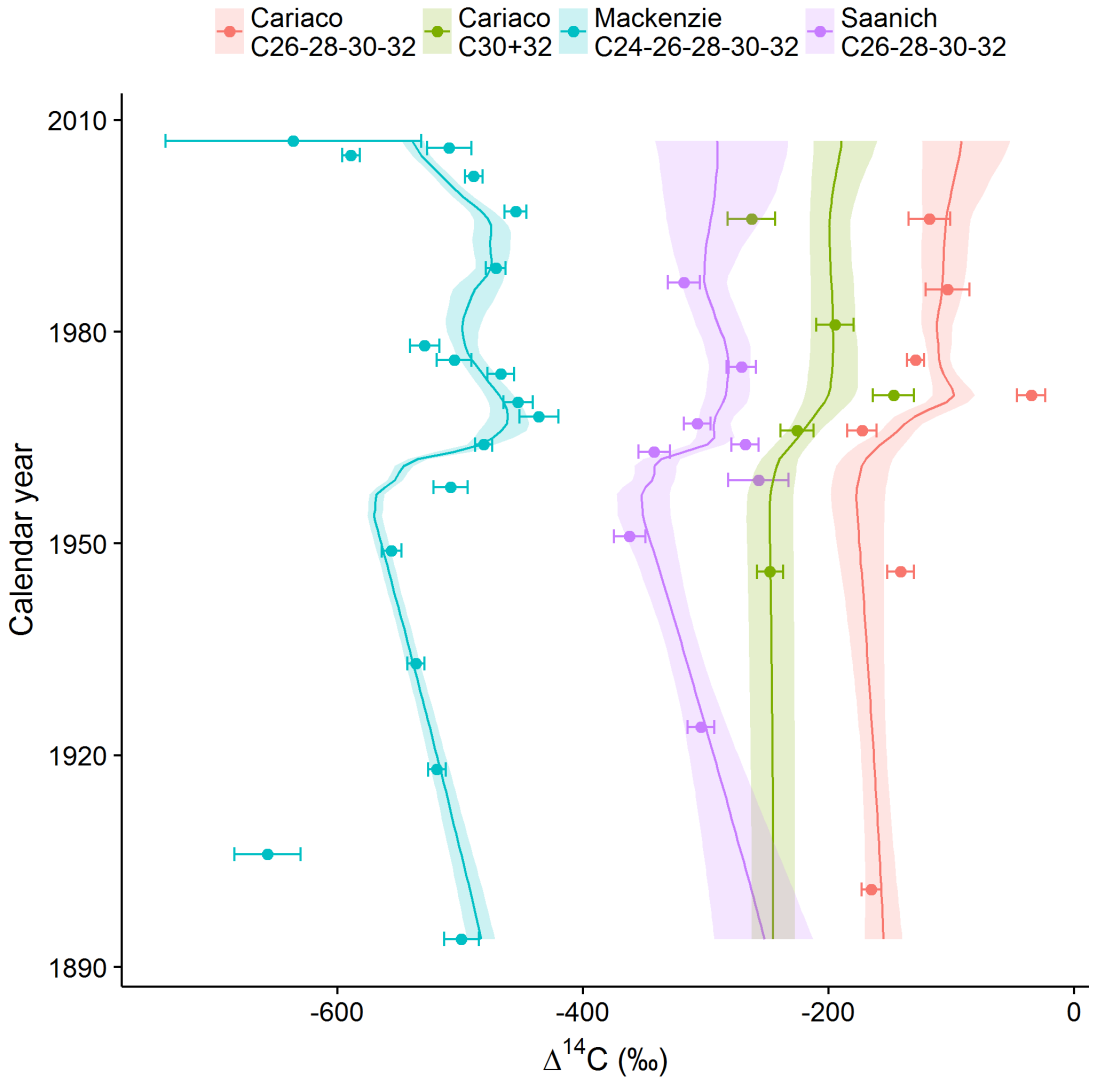

Figure 8

Estimated predictive distribution of residence times τ (in years) less than 50 years against relative contribution of leaf wax derived fatty acids. The red line corresponds to an estimated initial uniform distribution that we chose to set in order to compare between sites. The Mackenzie Delta data are of sufficiently high resolution to "modify" that initial value. The Saanich Inlet and Cariaco Basin, however, show a clear pattern for the first 30 years but the lack of data points results in distributions that approach the estimated value beyond ca. 30 years, meaning that our model predictions are not reliable for this interval.

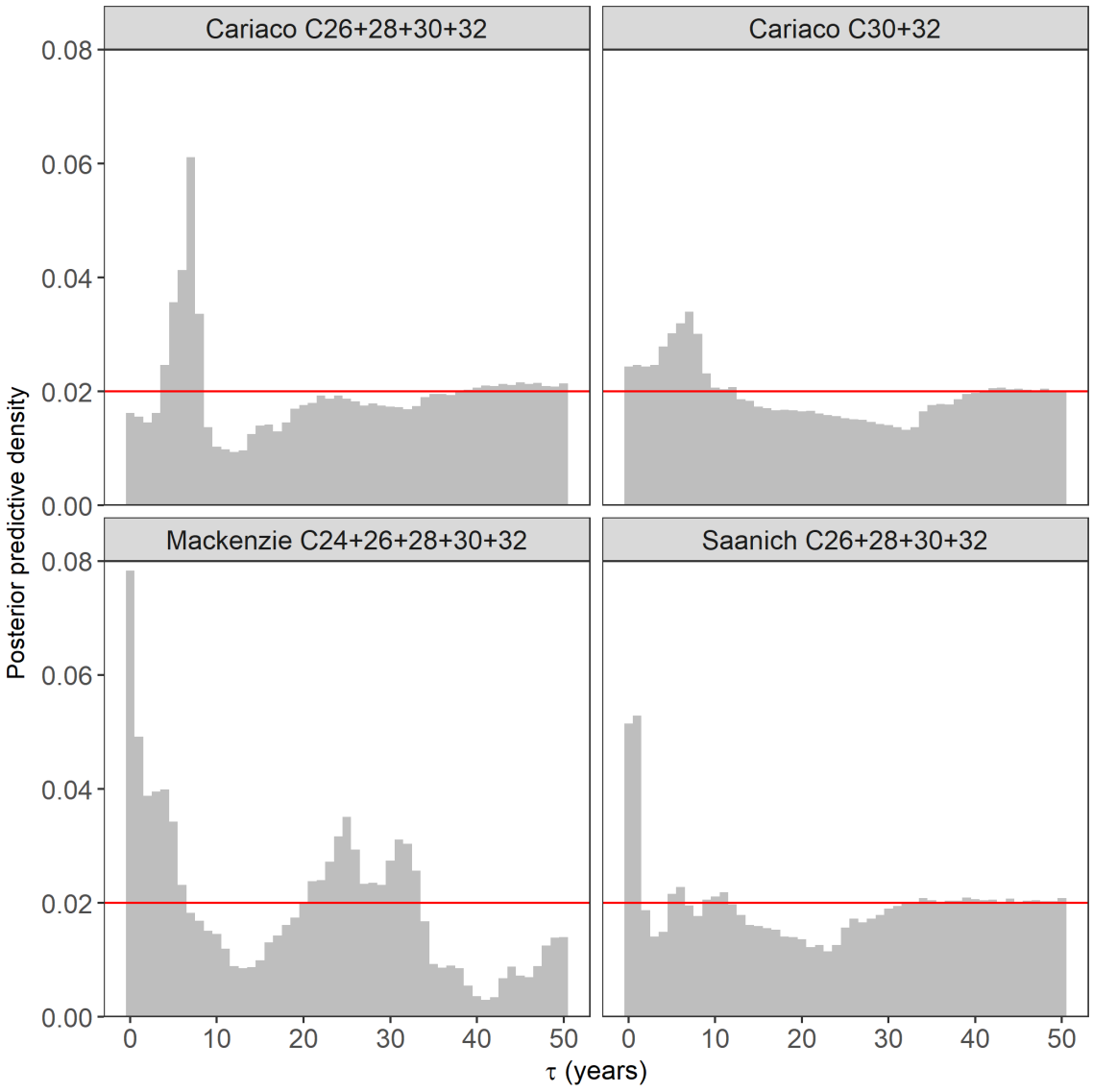

Figure 9

Estimated parameter densities for (a) fraction old (f_{Old}), (b) the slope of the linear term *b* correcting for trends observed prior to the bomb-spike (not applied for Cariaco C_{30}-C_{32}), and (c) residence time of the old pool (τ_{Old}). Note the logarithmic axis scale of τ_{Old}.

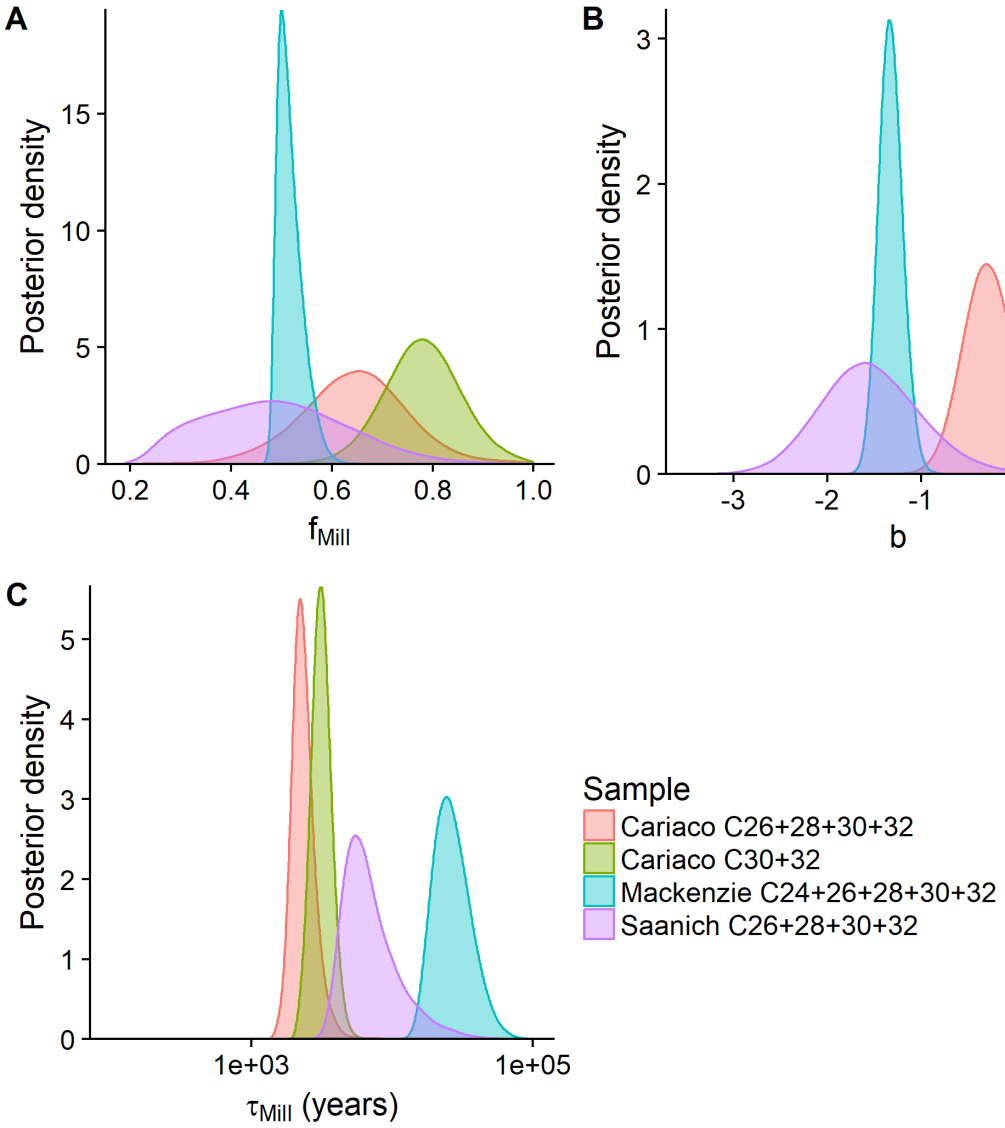

Supplemental Online Material

Table S1

Concentrations of long-chain *n*-alkanoic acids in core MK09#2 of the Mackenzie Delta. Note that n.a. is "not analyzed" and n.d. is "not detectable".

	Long-chain *n*-alkanoic acids concentrations (µg/gOC)														
Depth (cm)	**16**	**17**	**18**	**19**	**20**	**21**	**22**	**23**	**24**	**25**	**26**	**27**	**28**	**29**	**30**
0.5	16	1.1	4.0	0.51	3.1	2.1	8.9	4.1	12	3.0	9.0	1.7	7.3	1.0	3.2
1.5	100	4.6	16	1.9	18	5.2	28	9.8	33	7.7	22	3.3	13	2.6	6.1
4.5	n.a.	n.a.	n.a.	n.a.	n.a.	n.a.	18	n.a.	31	n.a.	23	n.a.	20	n.a.	n.a.
20.5	12	0.79	3.1	0.38	2.4	1.6	6.7	3.1	9.0	2.3	6.8	1.2	5.5	0.77	2.5
32.5	n.a.	n.a.	n.a.	n.a.	n.a.	n.a.	16	n.a.	27	n.a.	20	n.a.	17	n.a.	n.a.
40.5	13	0.58	2.1	0.23	1.7	0.75	3.4	1.3	3.8	0.83	2.3	0.41	2.1	0.19	1.1
41.5	9.2	0.16	1.2	0.18	2.3	0.69	3.5	1.3	3.2	0.90	1.8	n.d.	1.1	n.d.	1.6
52.5	n.a.	n.a.	n.a.	n.a.	n.a.	n.a.	19	n.a.	25	n.a.	19	n.a.	18	n.a.	n.a.
60.5	12	0.54	2.3	0.20	1.5	0.67	2.8	1.1	2.9	0.65	1.5	0.27	2.1	n.d.	1.2
80.5	4.1	0.20	0.76	0.075	0.68	0.36	1.6	0.57	1.6	0.36	1.1	0.20	0.82	0.10	0.41
81.5	39	1.6	7.0	0.76	7.0	1.8	9.2	3.1	7.8	2.1	5.0	0.67	3.6	n.d.	n.d.
84.5	n.a.	n.a.	n.a.	n.a.	n.a.	n.a.	46	n.a.	93	n.a.	75	n.a.	64	n.a.	n.a.

Table S2

Concentrations of fatty acids (in µg/gOC) at Cariaco Basin and Saanich Inlet. Both sites show bimodal abundance of chain lengths, with maxima at nC_{16} and nC_{24}-nC_{26} reflecting contributions from algal/bacterial cell walls and higher plant leaf waxes, respectively.

Cariaco Basin	**fatty acid concentrations in µg/gOC**									
Deposition year	***n*C$_{14}$**	***n*C$_{16}$**	***n*C$_{18}$**	***n*C$_{20}$**	***n*C$_{22}$**	***n*C$_{24}$**	***n*C$_{26}$**	***n*C$_{28}$**	***n*C$_{30}$**	***n*C$_{32}$**
1901	62.6	105	42.4	16.4	31.8	96.1	94.5	30.3	20.7	21.3
1946	74.3	107	46.5	17.5	27.1	94.8	73.5	20.3	11.8	7.4
1956	161	587	115	36.9	32.9	50.9	51.1	34.5	30.8	22.1
1961	188	639	224	47.3	51.5	86.2	95.7	54.8	14.7	29.1
1966	47.5	129	25.4	22.2	41.7	128	146	29.9	18.2	23.6
1971	62.3	112	52.6	23.1	50.1	156	170	32.7	20.1	14.8
1976	143	219	82.8	23.7	33.6	101	110	25.0	26.9	10.4
1981	44.7	132	61.2	22.8	48.5	157	152	31.6	22.0	27.6
1986	116	329	81.7	29.6	35.3	94.4	95.7	25.6	16.5	13.2
1991	428	944	224	155	145	366	269	65.3	86.2	26.0
1996	135	193	37.8	32.5	64.7	151	102	29.4	22.8	28.1
Saanich Inlet										
Deposition year	***n*C$_{14}$**	***n*C$_{16}$**	***n*C$_{18}$**	***n*C$_{20}$**	***n*C$_{22}$**	***n*C$_{24}$**	***n*C$_{26}$**	***n*C$_{28}$**	***n*C$_{30}$**	***n*C$_{32}$**
1924	166	395	74.6	29.9	79.0	192	132	72.3	51.0	20.2
1951	201	461	81.9	20.5	54.0	120	89.9	59.3	44.1	18.7
1959	113	235	63.7	31.1	98.1	203	152	119	83.8	41.4
1962	133	340	82.2	31.7	88.4	170	106	70.7	50.5	21.9
1963	181	475	94.4	29.0	77.2	149	94.9	58.1	34.8	16.3
1964	162	318	73.0	28.4	79.3	145	97.9	69.0	44.7	19.0
1967	238	529	89.6	36.4	113	201	138	101	70.6	36.6
1971	117	271	107	39.5	114	204	139	103	76.7	31.7
1975	164	373	138	49.6	120	211	144	99.7	71.6	36.0
1987	275	518	120	54.1	124	207	118	78.6	62.3	32.5

Table S3a

Compound-specific ^{14}C data for fatty acids in Cariaco Basin and Saanich Inlet sediments. Sample size for ^{14}C analyses (in µg) is reported within brackets. Asterisk (*) mark the values that are not based on direct AMS measurements, but are calculated as concentration-weighed ^{14}C values of individual compounds, in order to compare with other locations.

Cariaco Basin							
Year	**C_{16}**	**C_{24}**	**C_{26}**	**C_{28}**	**C_{30+32}**	**$C_{26+28+30+32}$**	**$C_{24+26+28+30+32}$**
1901	22±14 (43)					-165±8 (72)	
1946	-84±11 (61)	-159±11 (82.1)	-56±8 (73.3)	-231±20 (21.5)	-248±11 (40.4)	-141*	-148*
1956	-40±65 (9.3)						
1961	-21±61 (9.8)						
1966	3±14 (45)	-141±11 (72.1)	-153±10 (67.4)	-153±22 (21.3)	-226±13 (32.8)	-173*	-161*
1971	-11±12 (50)	21±10 (101)	10±10 (79)	-50±24 (21.5)	-147±17 (28.7)	-35*	-10*
1976	52±14 (51)	65±18 (32.4)				-129±7 (63)	
1981	76±15 (51)	93±12 (102)	19±10 (68.9)	-92±25 (19.8)	-195±15 (30)		14*
1986	90±193 (4.8)	-624±11 (34.4)				-103±18 (27)	
1991	88±135 (5.9)						
1996	1±12 (64)	-74±15 (69.5)	-29±15 (15)	-194±31 (15.4)	-263±19 (23.1)	-118*	-99*
Saanich Inlet							
Year	**C_{16}**	**C_{24}**	**C_{26}**	**C_{28}**	**C_{30+32}**	**$C_{26+28+30+32}$**	**$C_{24+26+28+30+32}$**
1924	-81±21 (31)	-93±22 (23)				-304 (38.7)	-225*
1951	-117±16 (32)					-362 (29.8)	
1959	1±85 (7.8)	-120±21 (23)	-223±22 (20)	-268±35 (13)	-290±28 (15.9)	-257*	-212*
1963	-56±18 (34)	-58±24 (21)				-342 (30.9)	-94*
1964	5±15 (37)	132±19 (26)				-268 (38)	-213*

1967	-2±15 (41)	-72±26 (19.4)			-307 (36.1)	-225*
1971	-210±40 (12)	-49±23 (22.4)	-190±41 (12)	-224±32 (14.8)		
1975	-33±58 (10)	-110±27 (18.7)			-271 (34.4)	-214*
1987	-10±17 (33)	-124±24 (20.6)			-318 (31.1)	-241*

Table S3b

Compound-specific ^{14}C data for fatty acids in Mackenzie Delta sediments. Sample size for ^{14}C analyses (in µg) is reported within brackets.

Year	$C_{24+26+28+30+32}$
2006	-509±18 (8.8)
2007	-636±104
2005	-589±6.8
2002	-489±7.5
1997	-455±8.7
1989	-471±8.3
1978	-529±12 (14.4)
1976	-505±14 (12.8)
1974	-467±11
1970	-453±12 (16.8)
1968	-436±16 (12.0)
1964	-481±6.5
1958	-508±14 (12.8)
1949	-556±7.6
1933	-536±6.8
1918	-519±7.4
1906	-657±27
1894	-499±14 (-12.0)

Table S4: Estimated mean and standard deviations (between brackets) of the estimated predictive distributions of parameters b, f_{old}, and τ_{Old} as well as the fractional contributions (0-2 years, 0-5 years, 0-10 years, and 10-50 years) for the Bay of Bengal fatty acid data from French et al. (2018). The young pool is operationally defined as <50 years, and all ages are reported in calendar years. Note that the young pool fractions consist of a total of 25-27% (1-f_{Old}), but are presented as a total contribution of 100%. Note that for the C28 model run, the 1975 data point was treated as an outlier.

	Old pool contributions/age (y)		**Young pool contributions/age (y)**				
	f_{Old}	τ_{Old}	**0-2**	**0-5**	**0-10**	**10-50**	**b**
Bay of Bengal C24-26-28-30-32	0.73 (0.02)	1332 (76)	0.01 (0.01)	0.05 (0.02)	0.19 (0.03)	0.81 (0.03)	0
Bay of Bengal C28	0.75 (0.04)	1313 (152)	0.07 (0.03)	0.11 (0.04)	0.28 (0.05)	0.72 (0.05)	0

Figure S1

Bulk geochemical data for Cariaco core #MC5 (red), Saanich core #SI3 (blue) and Mackenzie core MK07#6 (green circles) sediments, with (a) TOC in weight %, (b) TOC/TN ratios, (c) $\delta^{13}C_{TOC}$ (‰), and (d) $\Delta^{14}C_{TOC}$ (‰) plotted against calendar year (AD). Mackenzie data are from Vonk et al. (2016) and Cariaco and Saanich data are from Drenzek (2007).

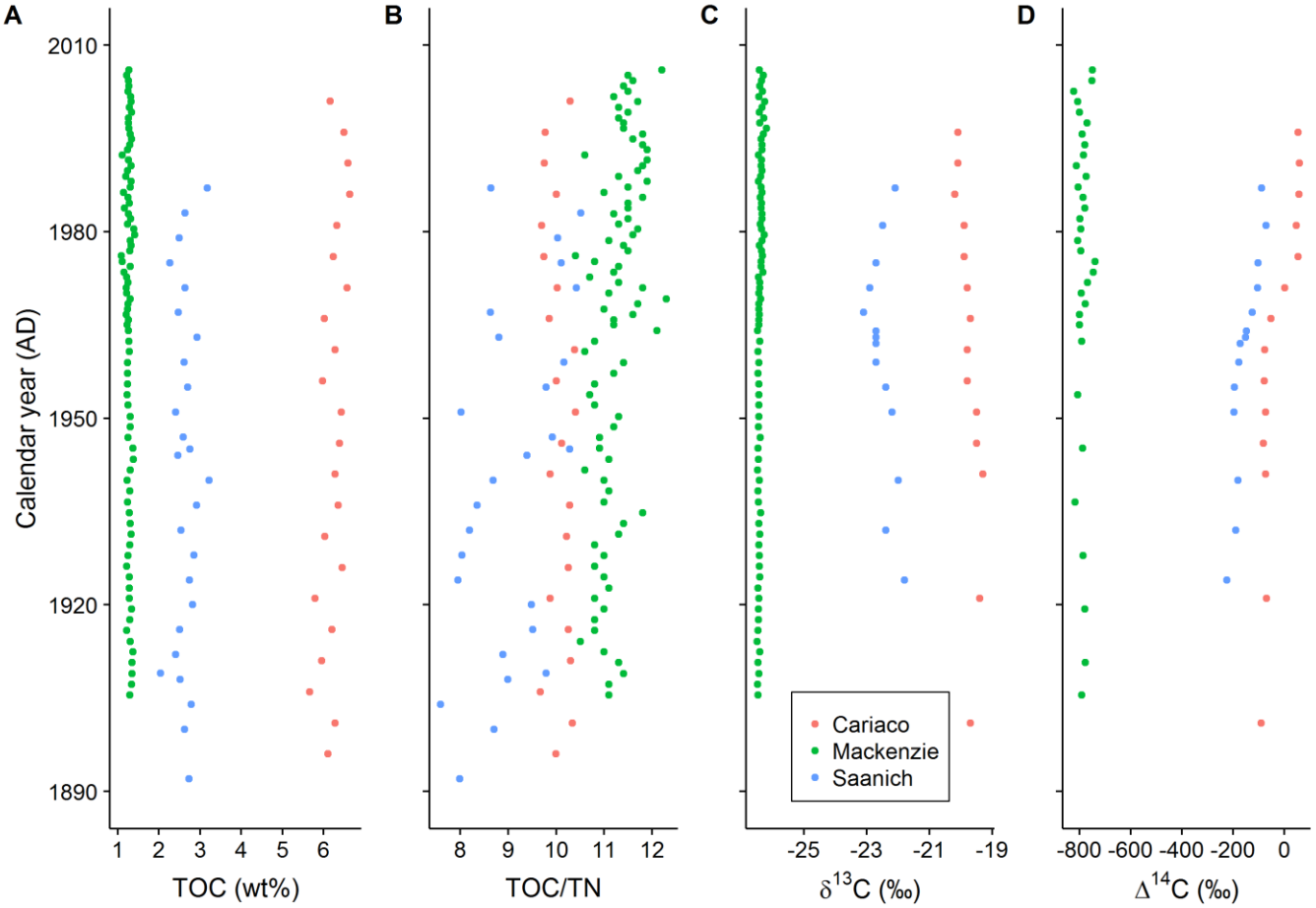

Figure S2

Fatty acid $\delta^{13}C$ compositions extracted from (a) Cariaco Basin and (b) Saanich Inlet sediments, color-coded for year of deposition. Errors represent 1σ analytical uncertainties from triplicate GC/IRMS measurements.

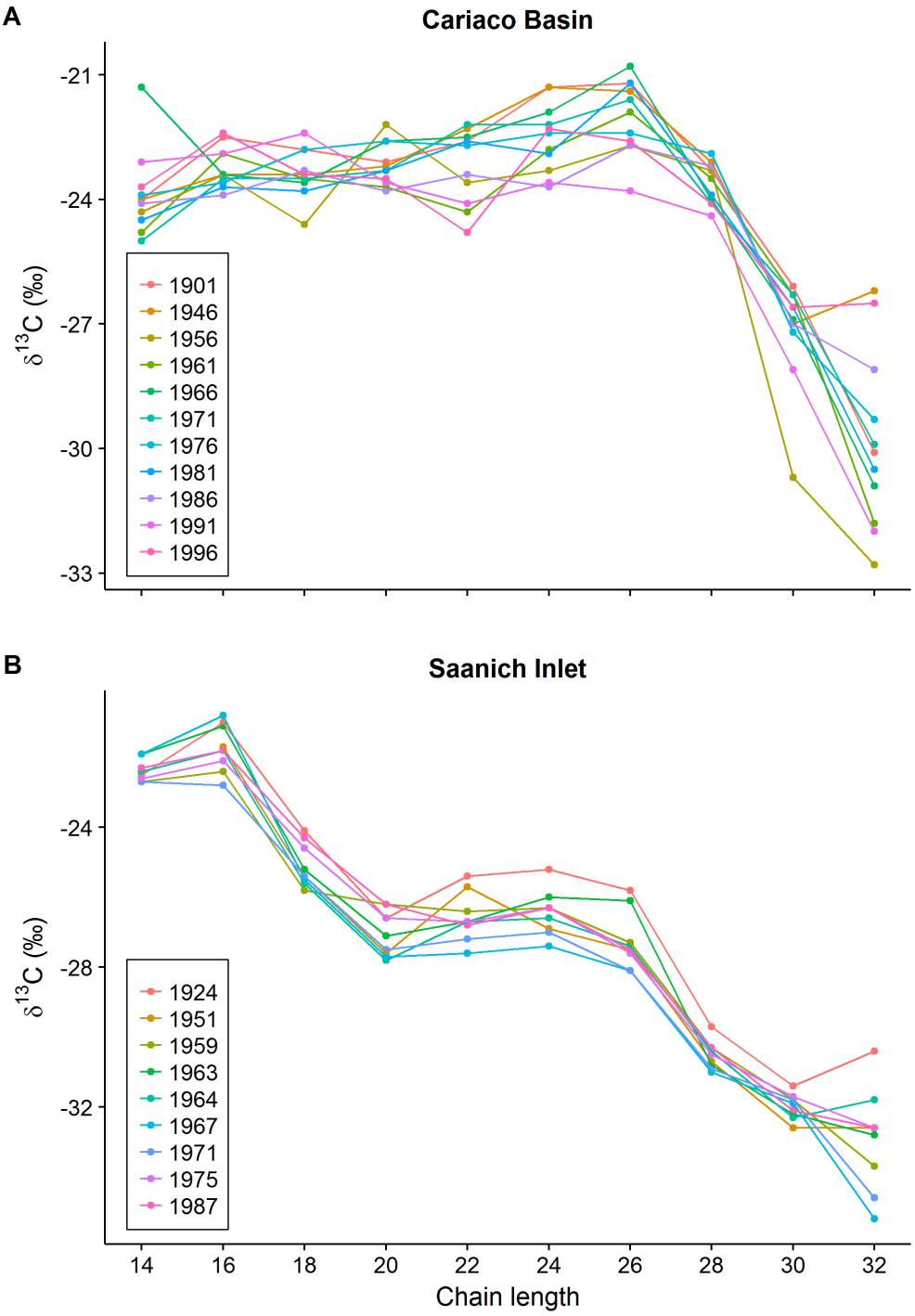

Figure S3

Fatty acid long-chain ^{14}C composition of nC_{16} for Cariaco Basin (white circles) and Saanich Inlet (black circles). The ^{14}C composition of nC_{16} was not analyzed for the Mackenzie Delta.

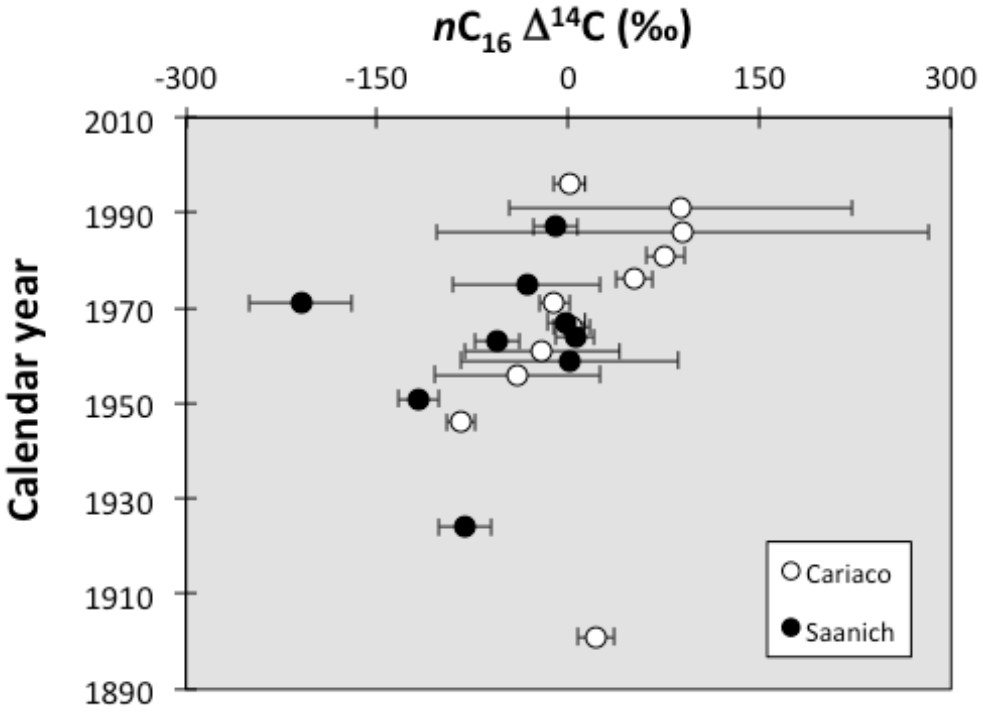

Figure S4

Predictive distribution of residence times τ (in years) less than 50 years against relative contribution of leaf wax derived fatty acids at Cariaco Basin (upper), Mackenzie Delta (middle) and Saanich Inlet (lower graphs). The graphs on the left are based on full data and the graph(s) on the right after removing outlying data point from 1959 (Cariaco Basin), 1906, 1978, 2005 (Mackenzie Delta), and 1971, 1976 (Saanich Inlet). For Cariaco Basin $C_{26+28+30+32}$, the sequence of observations from 1966, 1971 and 1976 shows a rise followed by a sharp decline in $\Delta^{14}C$ (Fig. 6a) that can not be matched by the more gradual decline of the atmospheric CO_2 signal. Removing either the 1971 or the 1976 data-point gave results free from outliers and qualitatively similar results as for full data regarding parameters f_{Old}, b and τ_{Old} (Fig. S8). However, when removing the 1971 observation the sharp peak in the relative proportion of age ≈7 year material vanishes.

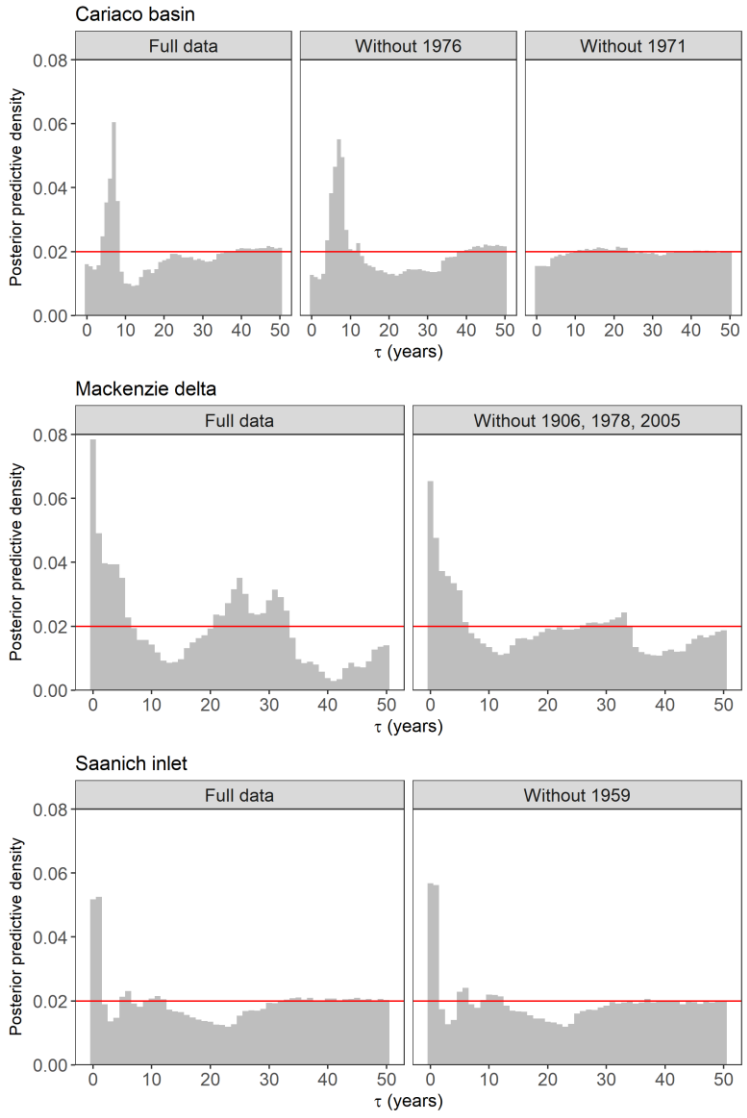

Figure S5

Estimated parameter densities from Saanich Inlet, with and without inclusion of outliers.

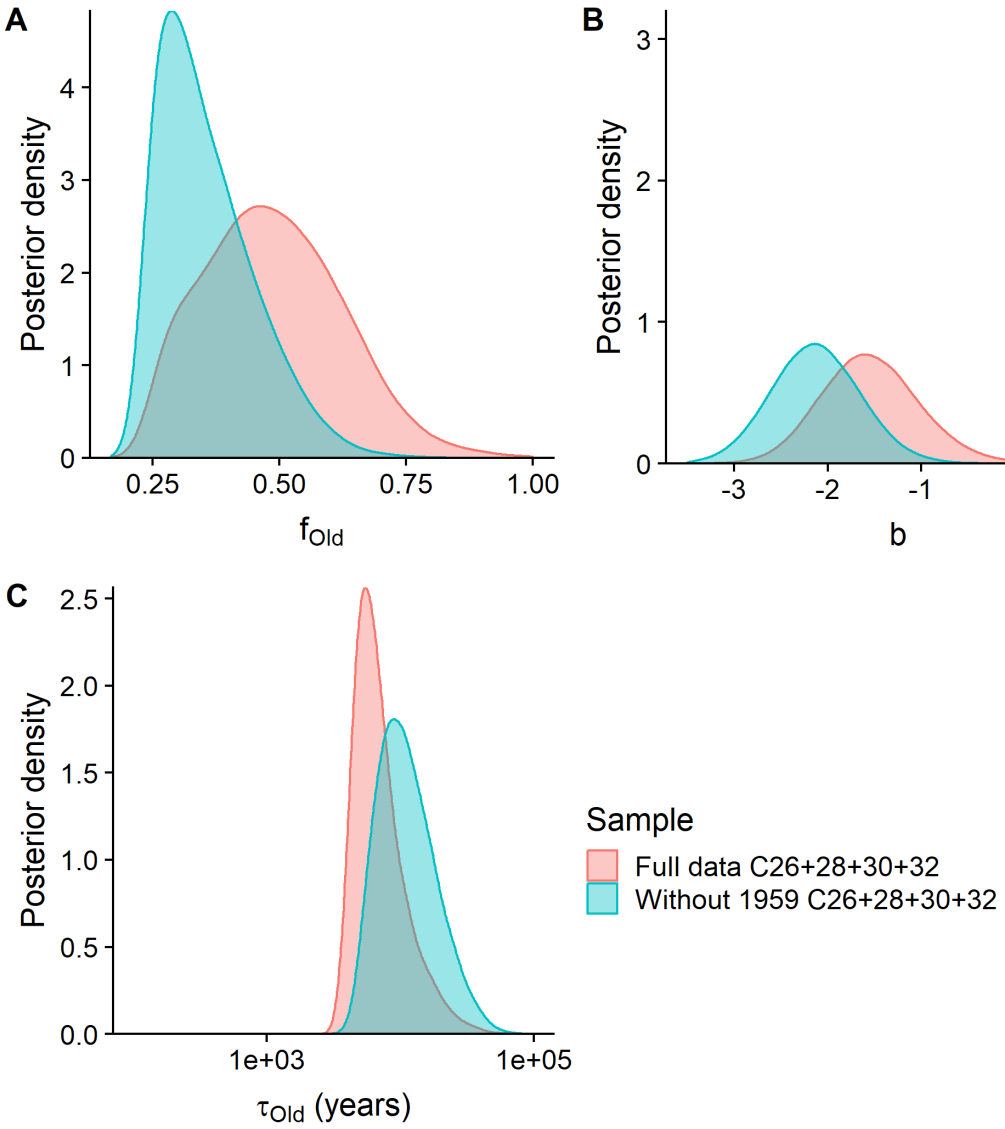

Figure S6

Estimated parameter densities from Mackenzie Delta, with and without inclusion of outliers.

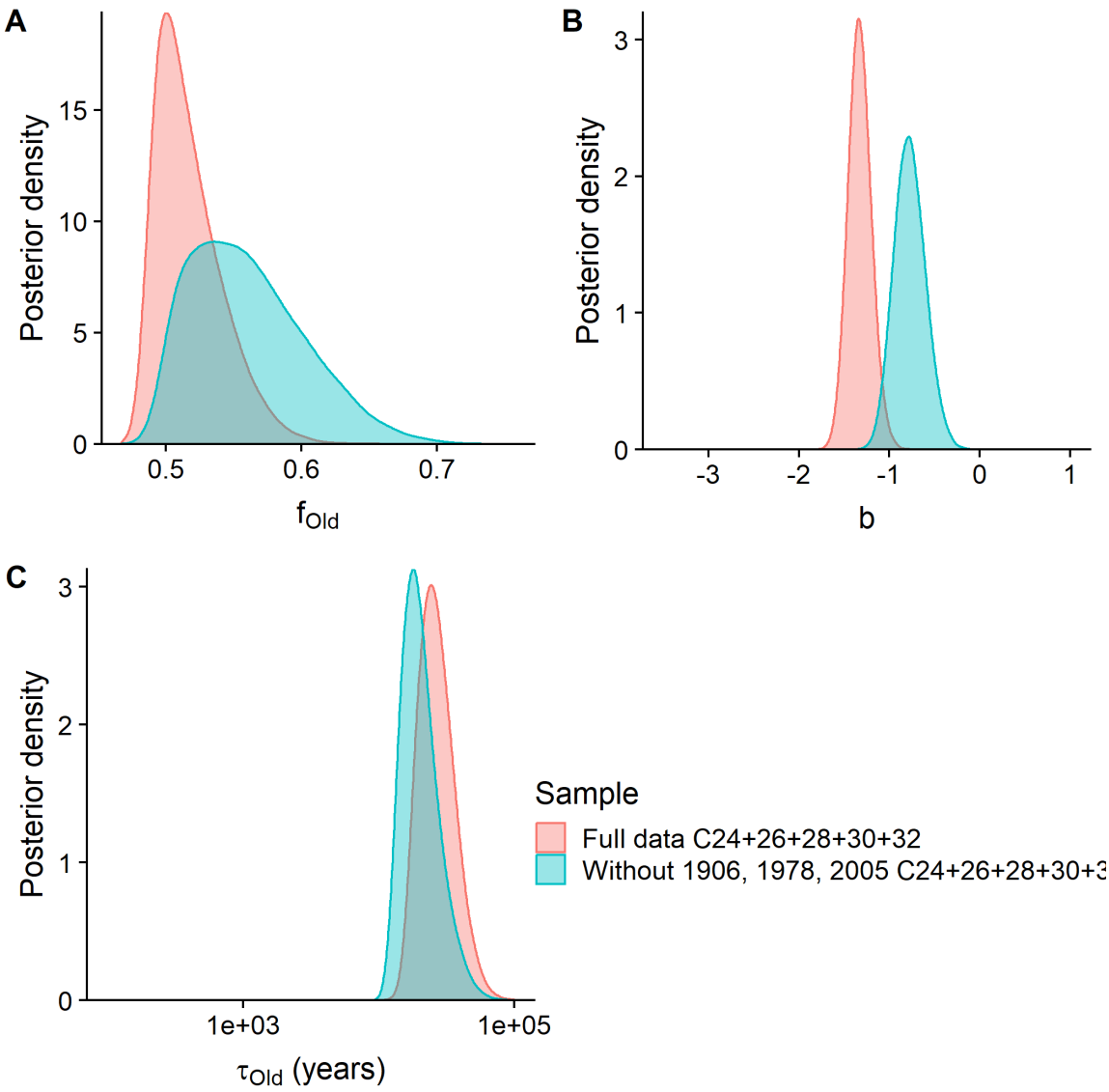

Figure S7

Estimated parameter densities from Cariaco Basin, with and without inclusion of outliers.

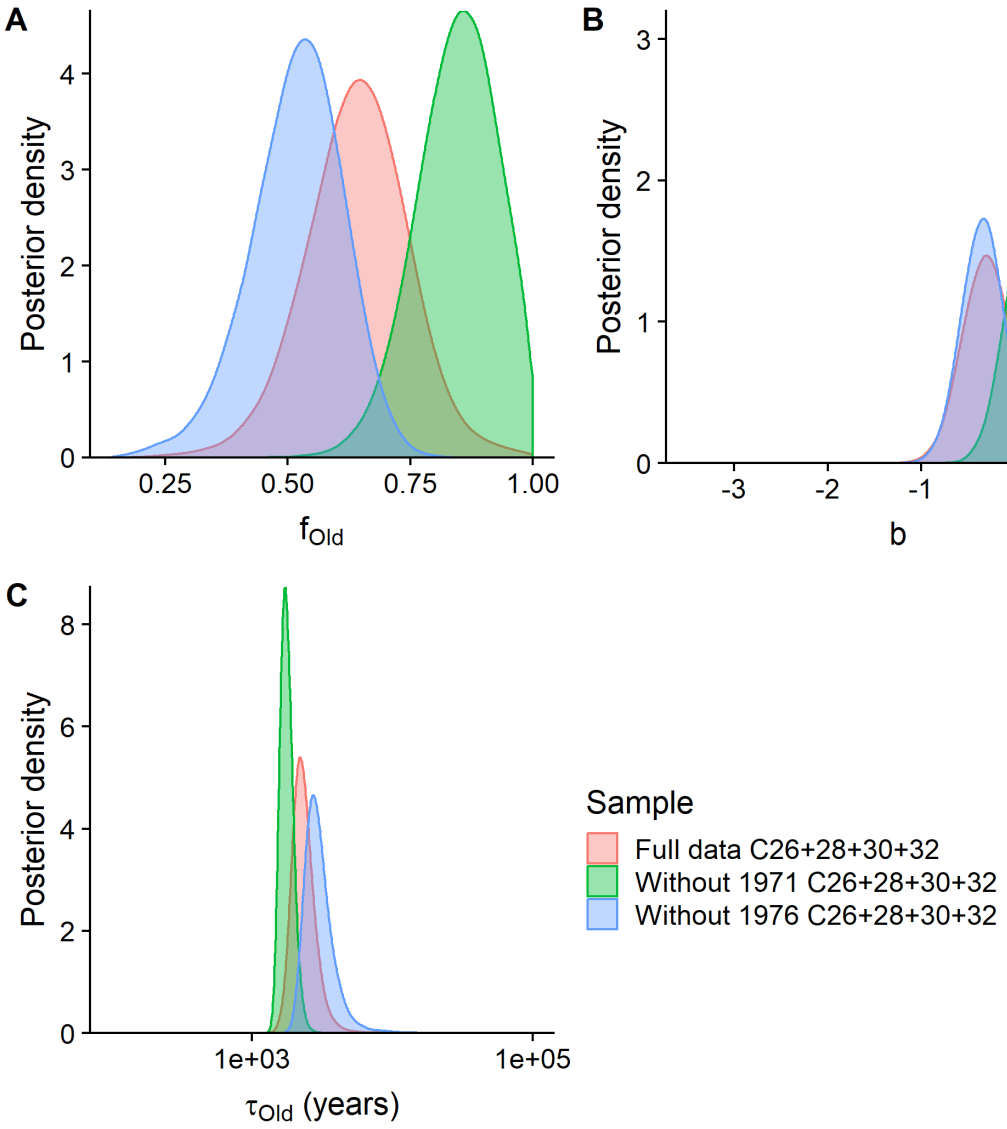

Figure S8

Model fits of estimated mean $\Delta^{14}C_{obs}(t)$ from equation [4] without parameter b. The lines include a 90% credible interval and data, against calendar year in sediment cores, with (from left to right) Mackenzie Delta (light blue, $nC_{24+26+28+30+32}$), Saanich Inlet ($nC_{26+28+30+32}$), and Cariaco Basin (green, nC_{30+32} and red, $nC_{26+28+30+32}$). All data points are included in the model fit.